Metabolic engineering of isoprenoid biosynthesis in *Synechococcus elongatus* PCC 7942

Zachary D. Wiltshire

A Thesis
in
The Department
of
Biology

Presented in Partial Fulfillment of the Requirements
for the Degree of Master of Science (Biology) at
Concordia University
Montreal, Quebec, Canada

June 2016

CONCORDIA UNIVERSITY
School of Graduate Studies

This is to certify that the thesis prepared

By: Zachary D. Wiltshire

Entitled: Metabolic engineering of isoprenoid biosynthesis in *Synechococcus elongatus* PCC 7942

and submitted in partial fulfillment of the requirements for the degree of

Master of Science (Biology)

complies with the regulations of the University and meets the accepted standards with respect to originality and quality.

Signed by the final examining committee:

_____ Chair
Dr. Grant Brown

_____ External Examiner
Dr. David Walsh

_____ Examiner
Dr. William Zerges

_____ Examiner
Dr. Luc Varin

_____ Supervisor
Dr. Vincent Martin

Approved by: _____
Dr. Grant Brown, Graduate Program Director

_____ _____
Date Dr. André Roy, Dean of the Faculty of Arts and Sciences

Abstract

Metabolic engineering of isoprenoid biosynthesis
in *Synechococcus elongatus* PCC 7942

Zachary D. Wiltshire

The feasibility of increasing isoprenoid biosynthesis in the obligate photoautotrophic cyanobacterium *Synechococcus elongatus* PCC 7942 was explored through the use of a heterologous mevalonate pathway. Incorporation of heterologous genes that produce non-native metabolic intermediates has previously been demonstrated as a method of increasing product formation while bypassing endogenous regulatory mechanisms. While this design strategy has been exhaustively explored in model heterotrophic microbes, far less work has been carried out in photoautotrophs. Practically, this disparity is due to the preference of using faster growing heterotrophs, greater understanding of metabolic regulation in model heterotrophs, and more limited characterisation of genes and genetic regulatory elements in cyanobacterial hosts (particularly *S. elongatus*). Here the host response to incorporation of a heterologous mevalonate pathway under the control of non-native promoters is characterised. Analysis was focused on metabolic intermediates, endogenous isoprenoid products, and cell growth indicators, primarily using HPLC and GC-MS. The heterologous route for isoprenoid biosynthesis was found to be functional. An intermediate in this pathway, mevalonate, accumulated to 70μM under standard laboratory conditions. Recorded changes to endogenous isoprenoid products were smaller, but still apparent. Because of commercial interest in phototrophic production of isoprenoids, particularly for fuels, I also attempted to generate a previously demonstrated biofilm phenotype in *S. elongatus*. This phenotype is of interest for testing in evanescent field based photobioreactors, but I was unable to replicate it during the period of work.

Acknowledgements

I want to extend my thanks to past and current members of the Martin and Walsh labs for their support and friendship. There was always someone willing to provide advice, whether technical or personal. I would also like to acknowledge the support of my committee members. I particularly want to acknowledge my supervisor Dr. Vincent Martin who provided an enormous amount of leeway and support for me to pursue side projects, including involvement with the iGEM program and Hyasynth Bio. And of course my family and friends for their constant love, support, and belief in me.

Table of Contents

List of Figures

List of Tables

List of Equations

List of Abbreviations

2YT	Yeast extract/tryptone based growth medium
$Abs_{\#nm}$	Absorbance measurement at the indicated wavelength (OD - "optical density")
ATP	Adenosine triphosphate
BG-11	Blue-green medium #11
bp	Base pairs
CDS	Coding sequence
CRISPR-Cas	Clustered regularly-interspaced short palindromic repeats - CRISPR associated gene
DOXP pathway	1-deoxy-D-xylulose 5-phosphate pathway (see MEP pathway)
FS	α-Farnesene synthase
GC-MS	Gas chromatography mass spectrometry
HPLC	High performance liquid chromatography
IPTG	Isopropyl β-D-1-thiogalactopyranoside
LB	Lysogeny broth
MEP pathway	2C-methyl-D-erythritol 4-phosphate pathway (Non-mevalonate pathway; also known as DOXP pathway)
MVA pathway	Mevalonate (Mevalonate pathway)
$NADH/NAD^+$	Reduced/oxidised forms of nicotinamide adenine dinucleotide
$NADPH/NADP^+$	Reduced/oxidised forms of nicotinamide adenine dinucleotide phosphate
NS#	*S. elongatus* neutral site for genomic integration
PCC	Pasteur Culture collection of Cyanobacteria
Sa	*Staphylococcus aureus*
S. elongatus	*Synechococcus elongatus* PCC 7942
Synechocystis	*Synechocystis* sp. PCC 6803
Synpcc7942_#	*S. elongatus* gene reference number

Goal and Objectives

This work aims to explore metabolic engineering of the cyanobacterium *Synechococcus elongatus* PCC 7942 (*S. elongatus*) for increased isoprenoid production. Isoprenoids are a diverse class of molecules with many uses including fuel, fragrances, health products, and as flexible chemical building blocks for synthetic products. *S. elongatus* is photoautotrophic, enabling direct-from-CO_2 (photosynthetically-fixed carbon based) production of these molecules.

Currently, many of these isoprenoids are derived from expensive plant sources or environmentally damaging petroleum products. Carrying out photofermentation of engineered microbes has the potential to increase product yield, decrease losses to side product formation, and sequester the atmospheric greenhouse gas, carbon dioxide.

Production of desired isoprenoids can be improved by manipulating the host cell's metabolism. Two distinct metabolic pathways can carry out isoprenoid biosynthesis. One of these pathways is found natively in *S. elongatus*. I introduced the non-native version of this pathway in two parts into *S. elongatus* and examined the resulting metabolic changes to the host. The changes examined included metabolism of both native and foreign metabolites, as well as metabolic burden resulting from added genes.

Improvements to molecule production in photoautotrophic microbes like *S. elongatus* can be sometimes negated by poor industrial photobioreactor design, particularly for low cost products like fuels. To complement the metabolic engineering carried out, I briefly explored biological design considerations for the growth of *S. elongatus* in higher efficiency evanescent field based bioreactors.

Taken together, improvements in metabolic efficiency and growth at production scales have the potential to enable economically efficient synthesis of commodity and specialty chemicals with a decreased environmental impact compared to traditional industrial methods.

Introduction

Metabolic engineering

Metabolic engineering, and the related field of synthetic biology, are quickly becoming a major contributor to industrial chemical synthesis. It has been estimated that biologically produced chemicals will compose 10% of global chemical production by the year 2020.[1] Even without considering petroleum fuels, nearly 90 million metric tons of organic chemicals and lubricants are produced annually in the United States.[2] Bioproducts can enter this market as ready-to-use chemicals, platform molecules for further synthesis, functional biopolymers, and mixed pools of biomolecules for processing into functional products.[3]

Metabolic engineering, often using synthetic biology tools, is the cellular design process that is creating economically viable systems for producing these bioproducts. Early metabolic engineering efforts relied on slow and inadequate tools for rapid prototyping and, limited data on how genes and genetic regulatory elements behave in different contexts (host cell, plasmid, expression system). It is these problems that synthetic biology is attempting to remedy.[4]

Synthetic biology has developed into such a wide umbrella term for fields inside biological engineering that these names are often used interchangeably. At their core, these fields are working to introduce engineering rigour into biology that early "genetic engineering" only provided in name. New tools, particularly for DNA assembly, have increased the speed of the engineering design-build-test cycle in biology. Synthetic biology has yielded significantly more complex systems than its predecessor through the characterisation of genes and genetic regulatory elements, and the creation of novel (or rebuilt) biological systems, giving clearer insight into design guidelines for biological networks. As synthetic biology provides new tools and knowledge, metabolic engineering will continue to benefit.

Metabolic engineering's major focuses are improving existing metabolic systems (for a desired metabolite) and the creation of metabolism that does not exist in the cell being engineered.[5] Examples include biosynthesis of molecular precursors for therapeutics in bacteria and yeast, manufacture of polymer feedstocks, and microbial production of jet fuel.[6–9]

While not limited to microbial species, this is where a large majority of work has been carried out. Non-microbial targets are typically agricultural plants, which can be similarly grown on large scales.[10]

Economics, biology, and engineering of biofuels

Photosynthetic microorganisms have not seen the same widespread industrial adoption as obligate heterotrophs fed plant biomass for biofuel production. This has been partially due to historical industrial organisms (such as *Saccharomyces cerevisiae* - brewing yeast) having greater existing infrastructure, and because of the lower entry barrier for obtaining an economically viable strain.

S. cerevisiae strains naturally demonstrate significant ethanol production ability and tolerance to the ethanol produced. This trait is regularly employed at the largest industrial fermentation scales in the world for the production of fermented beverages, particularly beer.

While there are significant markets and distribution infrastructure for ethanol-containing beverages, ethanol biofuels have been mainly limited to major distribution in Brazil and in blends with traditional gasoline elsewhere. Ethanol biofuel production in Brazil is strongly incentivised by the high availability of sugarcane to use as a feedstock in heterotrophic fermentation. In the United States, economic viability of traditional heterotrophs has been artificially increased through the use of feedstock subsidies, particularly corn, in order to produce "greener" fuels. These subsidies have in some cases resulted in higher food costs and a decrease in the proportion of agricultural land use for food production.[11] Use of agricultural wastes (by themselves or from dedicated fuel crops,) that are high in lignocellulosic materials, will help decrease fermentation wastes and feedstock costs, and "green" the biofuel fermentation process further by more completely utilising the products of photosynthesis.

Algal biofuels

Because heterotrophic biofuels are generated by organisms consuming biomass generated by photosynthetic organisms, significant energy loss occurs in the transition from sunlight to fuel. Using a photosynthetic microbe (ie. a photosynthetic microalgae[A]) directly for the production of biofuels eliminates this second biomass generation step, and decreases the associated carbon emissions in the fuel generation process.

Algae can be used for biofuel generation in three main ways, with each method having been demonstrated at pilot or production scale:

- Growth as an alternative "crop" to feed heterotroph fermentation as described above.[12]
- Whole cell conversion by pyrolysis to "biocrude".[13,14]
- Secretion or accumulation of biofuel or biofuel precursor chemicals generated by engineering the algae's metabolism.[15]

When used as feedstock, cultivated microalgae reduces the complexity involved in using the total photosynthetic biomass. Unlike plants, the carbon-rich, degradation-resistant structural polymers lignin and cellulose are not found in microbial algae.[16]

The biocrude approach can readily use natural or engineered algae. These algae are typically highly lipid-rich eukaryotes. In this approach, more than 50% of dry cell weight can be converted into biocrude, and substantial amounts of nitrogen is left behind that can be processed for use in fertiliser.[17] In some cases, the environmental benefits of using a photosynthetic organism are lost because product yields may be substantially better when eukaryotic algae are fed heterotrophically. In an example using the mixotrophic green algae *Chlorella protothecoides*,

---

[A] Algae being a polyphyletic group consisting of organisms containing a photosynthetic apparatus (or ancestrally containing a functional plastid,) while lacking the structural features that characterise land plants. Organisms in this group include cyanobacteria, archaeplastidans (rhodophyta, chloroplastida/viridiplantae, glaucophyta), and a subset of the remaining Bikonts that underwent secondary endosymbiotic events. To distinguish single and multicellular algae, single celled species are often referred to as microalgae.[136]

when fed heterotrophically, lipid accumulation was nearly four times greater than during photoautotrophic growth.[18]

Production and secretion of liquid biofuels generally involve metabolic engineering to generate sufficient fuel yields. In some cases, natural metabolic process, such as those designed to combat environmental stress, can augment yields by helping redirect carbon flux.[19,20] Examples include ethanol secretion by *Synechococcus elongatus* PCC 7942 (*S. elongatus*) and free fatty acid generation by *Synechocystis* sp. PCC 6803.[21,22] Generally, secretion is preferred over accumulation because of decreased recovery and purification costs. When lipids are the target molecule, an accumulation approach can result in 30% of production costs going towards purification.[23]

Current limitations to photosynthetic approaches

The main drawbacks to using photosynthesis, rather than heterotrophic systems, include slower growth rates, more expensive/inefficient infrastructure required for large scale production facilities, and structural inefficiencies in the photosynthetic process such as energetic waste due to chlorophyll antenna size.[24]

Heterotrophic microbes display very rapid growth when nutrients are not limiting in their environment. Under optimal conditions, common laboratory *Escherichia coli* strains have doubling times of approximately eighteen minutes.[25] *Saccharomyces cerevisiae* are roughly 5.5 times slower at 100 minutes per optimal doubling.[26] Reported growth rates for common photosynthetic organisms are significantly slower still. *S. elongatus* has a typical doubling time of approximately 420 minutes.[27] Under heavily optimized conditions, the doubling time may be as low as 246 minutes.[28] A model eukaryotic algae, *Chlorella pyrenoidosa* doubles every 11 hours when grown photoautotrophically.[29] *Dunaliella* sp., investigated for carotenoid production, have recorded doubling rates of 15-20 hours.[30,31] Recently, *Synechococcus* UTEX 2973, a close relative of *Synechococcus elongatus* PCC 7942, was described by Yu *et al*. as having an optimised doubling time of only 114 minutes under autotrophic conditions.[28]

Growing algae under phototrophic conditions necessitates each cell have access to light. Raceway style ponds are the traditional growth system for microalgae, having been used for the

past 60 years.[32] They provide an inexpensive (depending on land cost,) low complexity growth system. Raceway pond efficiency as a bioreactor is directly proportional to their physical area and local climate. The density of the microalgal culture is limited by the ability of the raceway design to efficiently mix the culture and, the ability for light to penetrate into the culture.[33] Contamination is often cited as a concern with this type of open reactor design, but raceway designs remain one of the systems of choice for non-transgenic microalgae such as *Arthrospira* spp. (*Spirulina*) because of their ease of implementation.[34] Because raceway systems are an open reactor design, environmental biodiversity concerns are raised when transgenic algae are used. These concerns have lead some algal fuel companies to pursue the development of suicide systems for their strains that limit strain viability outside of their reactor systems.[35]

Closed reactor systems exist in a variety of formats, but are generally composed of interconnected tubing or panels that increase the photosynthetically productive surface area of the system. Further efficiency gains can be realised through the increased environmental control available in closed systems. However, these productivity increases come at a financial cost. The physical infrastructure of closed systems is more expensive than open ponds. Traditional fermentation tanks are generally not considered a viable option for scaled photosynthetic growth because of their very low surface area to volume ratio.

The economic viability of photobiofuels will benefit the most from new photobioreactor designs that increase cell density while maintaining light availability. One of the more novel approaches to this photobioreactor problem has been the use of waveguides designed for the efficient distribution of light to algal monolayers. In a traditional photobioreactor the surface tends to be too bright and the interior too dark, resulting in only a small percentage of the reactor volume maintaining optimal growth conditions. Using the evanescent field generated by waveguides to grow algal monolayers promises order-of-magnitude improvements in the proportion of maximally productive algae in the reactor. These productivity increases will be most notable where cyanobacteria are employed, due to their size. Their diameter corresponds to the 1µm optimal penetration depth of the evanescent field beyond the waveguide.[36] Eukaryotic algae can have a diameter ten times larger than this.[37,38]

Alongside improved growth regimes for photosynthetic microbes, improvements to photosynthesis may greatly improve photobiofuel economic viability. Significant energy loss occurs at every conversion step in oxygenic photosynthesis. Less than half of the incident sunlight is absorbed, and at most two-thirds of that absorbed energy can be converted to chemical energy in the photosystems.[24] Further energy loss occurs at the point of molecular hydrogen generation. When energy loss due to metabolism for biomass accumulation is factored in, the highest possible total energy conversion efficiency from sunlight is only 10%.[24] When cells are placed in light conditions that exceed the system's photosynthetic ability, mechanisms such as non-photochemical quenching are employed to limit over-production of damaging reactive oxygen species. These type of issues are beginning to be addressed by improvements to light harvesting antenna, increased diversity of functional pigments, and enzyme/metabolism efficiency improvments.[24]

To investigate and improve metabolic inefficiencies in photosynthetic microbes, cyanobacteria have proven to be one of the best test systems. This is due to their simpler cellular organisation, earlier fully sequenced genomes, and the better stability of transformed strains.[39] Coupled with improved techniques for metabolic engineering, these reasons have resulted in a larger body of work of molecular studies applicable to metabolic engineering work.

Metabolic engineering in cyanobacteria

Only within the last decade have cyanobacteria become a production platform for metabolites outside their natural biochemistry. Endogenous metabolites targeted include biohydrogen and the carotenoids (Table 1).[40–43] Outside of this rudimentary biotechnological use of cyanobacteria, major studies with cyanobacteria have focused on ecological aspects, photosynthesis, and chronobiology.[44]

S. elongatus has been particularly important in moving chronobiology forward by allowing for more robust, large scale studies. Prior to the introduction of *S. elongatus*, generation of circadian clock mutants in various eukaryotes was haphazard and was coupled with a poor understanding of the underlying genetics.[45] While not evolutionarily related to the eukaryotic circadian clocks, the *S. elongatus* kaiABC system provided a simpler regulatory network that could be easily manipulated. Studies of kaiABC have supplied an excellent understanding of

oscillatory genetic circuit dynamics. The promoters related to this circuit have also been widely used historically for expression of genes in this and related species.[46]

S. elongatus and similarly named (but not directly related) freshwater cyanobacteria have become the focus of engineering efforts for a variety of commodity chemicals including endogenous chemicals, sugars,[47,48] other hydrophilic compounds,[49,48,50] and a wide variety of fuels (Table 1).

Carotenoids

Carotenoid production in algae has been investigated for decades (Table 1).[41–43,51] These endogenous compounds are of particular interest for the health food/supplement industry. Under certain stress conditions, particular natural algal strains have been measured to produce extreme quantities of carotenoids. β-carotene levels in *Dunaliella salina* were measured in one study to compose 40% of the culture's dry cell weight (DCW).[41] Although subsequent studies have not reported such high yields in *Dunaliella* sp., DCW yields between 3-10% have been reproduced.[42,51] However, it must be kept in mind that these yields generated in highly controlled systems are order(s) of magnitude higher than those reported at production scale.[51]

Hydrophilic commodity chemicals

Glucose

These hydrophobic endogenous chemicals provided an obvious starting point for the biotechnological use of algae (Table 1). The use of stress regimes has also allowed for the exploitation of underlying metabolic processes involving hydrophilic compounds. In *Synechococcus* spp., osmotic stress induced by high salt concentrations was shown to be managed by the production of sucrose as an osmolyte.[52–54] Utilising this natural metabolic process, Niederholtmeyer et al. (2010) converted *S. elongatus* into a sugar secreting microbial factory.[48] Their system involves enzymatic cleavage of the sucrose osmolyte into glucose and fructose, followed by facilitated diffusion out of the cell. This type of system contrasts directly with heterotrophic fermentation systems that require a reduced carbon (often sugar) input. The

use of the sugar secreting strain has been shown to support co-cultures at laboratory scale, and has even been proposed for use with artificial chloroplast/endosymbiotic systems.[48,55]

One reported problem with this system was a plateau reached in sugar concentration. Further investigation by the authors suggested this was due to biochemical and metabolic limitations inherent in the system as presented. The hexose sugar transporter employed was bidirectional and passive and, *S. elongatus* was only able to produce sucrose during the light phase of its diurnal cycle, likely consuming the hexose sugars during the dark phase.[48]

Sucrose

A similar study was carried out where *S. elongatus* was engineered to excrete sucrose directly. Yields were substantially higher with a final estimated titre of 2.6 g/L at a consistent rate of 36.1 mg/L/h. In a variety of the better environmental conditions reported in the study, sucrose production represented at least 40% of the biomass generated.[20]

Lactate

With another hydrophilic compound in *S. elongatus*, lactate, this concentration plateau was not observed, likely due to the secretion transporter chosen.[48] The lactate transporter, LldP, transports lactate using coupled transport driven by a proton gradient. During normal growth, *S. elongatus* can easily alkalise its growth medium to above pH 9, creating a proton gradient that can consistently export lactate. Lactate concentrations observed were roughly 2.5 times greater than the hexose sugars (Table 1). A similar engineering experiment in *Synechocystis* sp. PCC 6803, which did not include transporters, yielded lactate concentrations 3.2 mM (5x more than in *S. elongatus*.)[50]

Biofuels and polymers

Fuel production continues to be the most researched area for metabolic engineering in algae. For this reason, only examples in cyanobacteria will be discussed at length. This research boom has been driven by the need to generate energy production systems that can be used regionally for energy security and, to reduce the "carbon footprint" associated with the energy generation. The majority (but not all) have been chosen for their ability to function as "drop-in" fuels that do

not require modifications to the existing liquid fuel distribution and consumption systems. Criteria for being considered a drop-in fuel typically consist of having octane/cetane numbers similar to existing gasoline or diesel, the ability to blend with petroleum fuels over a wide range of concentrations, very limited hygroscopicity, and similar viscosity/gelling properties.[56]

Since many of these biofuels have chemical structures similar to the petroleum products they are designed to replace, they may also be utilised for processes beyond combustion just as petroleum products are. One of the most economically relevant of these uses is as precursor material for structural polymer synthesis. Example use cases include ethylene for the common thermoplastic polyethylene and isoprene for synthetic rubber.

Ethylene

Three well-studied enzymatic systems can facilitate ethylene biosynthesis, with two of these having been added to cyanobacterial hosts. The first, found in higher plants, is a two-enzyme process that uses 1-aminocyclopropane-1-carboxylic acid (ACC) synthase and ACC oxidase (ACS-ACO.) Ethylene synthesis through this route is dependent on methionine availability. These enzymes have been used in *Synechocystis* sp. PCC 6803 without any additional engineering, generating poor yields (10nl/ml/h/OD_{750}) (Table 1).[57]

The second pathway is bacterial and also methionine dependent. However, instead of proceeding through s-adenosylmethionine like ACS-ACO, 2-keto-4-methyl-thiobutyric acid (KMBA) is used.[58] Use of the bacterial KMBA enzymes have not yet been explored in cyanobacteria.

The third route, found in some bacterial plant pathogens (eg. *Pseudomonas syringae*,) is composed of a single enzyme, "ethylene forming enzyme" (EFE). EFE requires 2-oxoglutarate (2-OG), arginine, and dioxygen. This 2-OG dependent route is currently the most explored method for ethylene biosynthesis, particularly in cyanobacteria. Until recently, all ethylene work in cyanobacteria had focused only on the EFE (or ACS-ACO) enzyme(s) and environmental conditions. Productivity of EFE expressing strains could not be maintained beyond a few passages of the culture. Ungerer *et al.* improved the stability of EFE expression in *Synechocystis* sp. PCC 6803, leading to multiple order-of-magnitude yield improvements.[59] Further metabolic

engineering, focused particularly around 2-OG in the tricarboxylic acid cycle, has provided an additional 1.5-fold improvement to ethylene yield. At 7514µl/l/h, this represents >7% of the total carbon fixed by the cell.

Ethanol

While engineering for ethanol has been long carried out in heterotrophic microbes, particularly *S. cerevisiae*, work in algae for ethanol production began in 1999 (Table 1). Deng and Coleman's seminal paper entitled "Ethanol synthesis by genetic engineering in cyanobacteria" expanded the field of rational metabolic engineering for exogenous metabolites into the use of cyanobacteria.[21] Using a two-gene operon containing pyruvate decarboxylase and alcohol dehydrogenase II from *Zymomonas mobilis* they demonstrated total ethanol accumulation of up to 1.71mM by *S. elongatus*. Production was recorded with both the endogenous *rbcLS* and *E. coli* P_{LAC} promoters.

Butanol

Isobutyraldehyde is a biological precursor isobutanol production and other petroleum derived commodity chemicals. Atsumi *et al*. introduced genes for increased valine biosynthesis to *S. elongatus* to enable high level production of isobutyraldehyde.[60] Their maximum production of 723mg/l was higher than all similar systems in *S. elongatus* at the time of publication. When genes for isobutanol production were added, yield dropped to approximately 60% of the precursor total. These yields were shown to be related concentration limits for product toxicity in the host. 2-methyl-1-butanol was later demonstrated by similar means, using isoleucine biosynthesis for precursor production. Total yield only reached 200mg/l, with 2-methyl-1-butanol biosynthesis resulting in a lower toxicity threshold (Table 1).[61]

Fatty acids and alkanes

Continuous free fatty acid biosynthesis presents a challenge because of the need to decouple production from cell growth. Natural cyanobacteria with the highest lipid accumulation are typically under environmental stress, with a correspondingly slow growth rate. The most effective free fatty acid engineering in cyanobacteria has so far followed a similar methodology

to that used in *E. coli* (Table 1). The introduction of an acyl-acyl carrier protein (ACP) thioesterase (ACP-TE) converts an acyl-ACP molecule to the corresponding fatty acid.

In *Synechocystis* sp. PCC 6803, an *E. coli* ACP-TE was added along with modifications to weaken the cell wall, and knockouts to reduce diversion of carbon to side products. One of these knockouts eliminated diversion of acetyl-CoA to acetyl phosphate. Acetyl phosphate has been suggested to function as a global genetic response regulator in *Synechocystis* sp. PCC 6803.[62] Yields of secreted free fatty acids in this system (primarily C12/C14/C16) were as high as 197 mg/l.[22]

Targeted production of alkanes from fatty acid metabolism has been reported as high as 26 mg/l in *Synechocystis* sp. PCC 6803.[63] The dedicated enzymes taking fatty aldehydes to alkanes and alkenes were overexpressed and, enzymes diverting carbon away from fatty acid metabolism were knocked out. Newer single cell screening techniques for fatty acid/alkane production in cyanobacteria promise to increase the speed that new strains can be analysed.[64]

Isoprenoids and terpenoids

Lindberg *et al.* (2010) provided the first demonstration of metabolic engineering for isoprenoid fuels in cyanobacteria (Table 1). Using *Synechocystis* sp. PCC 6803, the authors introduced only an isoprene synthase and demonstrated isoprene production.[65] In a later study focused on bioreactor design using the same strain, the authors calculated that maximally 0.08% of fixed carbon was being partitioned into isoprene.[66] Bentley *et al.* (2014) continued this work with the addition of a heterologous mevalonate pathway to increase isoprenoid flux. Isoprenoid biosynthesis is described in detail in the section that follows. Over an eight-day growth period, the total isoprene generated was approximately 250μg/gDCW. This final strain was 2.5 times

more productive than the original with only the isoprene synthase.[67,B]

Limonene biosynthesis was demonstrated by Halfmann *et al*. (2014) in the filamentous cyanobacterium *Anabaena* sp. PCC 7120. In this study, the limonene synthase from the Sitka spruce was introduced into the cyanobacterium, along with genes for three rate limiting enzymes in the endogenous MEP isoprenoid pathway.[68] Photosynthetic production of farnesene was also very recently demonstrated in the filamentous cyanobacterium *Anabaena* sp. PCC 7120. Similar to the original work with isoprene biosynthesis in *Synechocystis* sp. PCC 6803, only the single gene required for synthesis of the final product was introduced. The authors recorded the rate of farnesene synthesis as 69.1µg/l/OD_{700}/day. Of interest in their results was a 60% increase in photosystem II activity when the farnesene synthase was expressed. (Photosystem II activity was also recorded to be higher in the limonene producing strain.) Although this filamentous, heterocyst-forming cyanobacterium is interesting for its ability to fix nitrogen, it is largely unexplored for industrial biosynthesis.

[B] In all three studies, the isoprene-synthase-only base strains were reported to result in the same isoprene yields when compared side by side.[67] This conflicts with the preliminary values presented in 2010. Assuming the 2014 data is correct, the 2010 isoprene yields were over-reported by 3.4 times. This discrepancy may be assigned to differences in growth conditions; in 2014 the strains were grown in the novel photobioreactor described in their 2012 study. Although along with improved isoprene harvesting, this reactor was designed specifically to increase the carbon available to the strains.

Table 1. Examples of microalgal derived products

Product		Organism	Total yield	Rate	Reference
Health Products					
Carotenoids:	β-carotene	*Dunaliella salina*	3 - 40% DCW		[51,41]
		Dunaliella bardawil	8% DCW		[42]
	Zeaxanthin	*Synechocystis* sp. PCC 6803	0.98 mg/l/Abs_{730}		[43]
Hydrophilic commodity chemicals					
Glucose/fructose		*Synechococcus elongatus* PCC 7942	250 µM (45 mg/l)		[47,48]
Sucrose		*Synechococcus elongatus* PCC 7942	(2.6 g/l)	36.1 mg/l/h	
Lactate		*Synechococcus elongatus* PCC 7942	620 µM (55 mg/l)	54 mg/l/day/Abs_{750}	[48]
		Synechocystis sp. PCC 6803	3200 µM		[50]
D-mannitol		*Synechococcus* sp. PCC 7002	(84.6 mg/l/OD_{730})	0.15 g/l/day	[69]
			1100 mg/l		
Biofuels and Polymers					
Hydrogen		*Synechococcus elongatus* PCC 7942			[40]([70])
Ethylene		*Synechococcus elongatus* PCC 7942	-	451 nl/ml/h/OD_{730}	[71] ([72])
		Synechocystis sp. PCC 6803	9739 µl/l/h (2-OG fed)	858 µl/ml/h/OD_{730} (fed)	[73] ([57,59])
			7514 µl/l/h (not fed)		
Ethanol		*Synechococcus elongatus* PCC 7942	1.71 mM	54 nmol/OD_{730}/l/day	[21]
		Synechocystis sp. PCC 6803	12 mM	5.2 mmol/OD_{730}/l/day	[74]
			9.8 mM		
Butanol:	2-methyl-1-butanol	*Synechococcus elongatus* PCC 7942	200 mg/l	20 mg/l/day	[61]
	Isobutyraldehyde	*Synechococcus elongatus* PCC 7942	723 mg/l	2.5 mg/l/h	[60]
Fatty Acid Derived:	Free FA	*Synechocystis* sp. PCC 6803	197 mg/l (secreted)	0.273 mg/l/h	[22]
		Synechococcus elongatus PCC 7942	49.3 mg/l	0.103 mg/l/h	[75]
		Synechococcus sp. PCC 7002	131 mg/l	0.438 mg/l/h	[76]
	Alkanes	*Synechococcus elongatus* PCC 7942	5% DCW		[77]
		Synechocystis sp. PCC 6803	26 mg/l (1.1% DCW)		[63]
			(2.3 mg/l/OD_{730})		[77]
Isoprenoids:	Isoprene	*Synechocystis* sp. PCC 6803	250 µg/gDCW	31 µg/gDCW/day	[65,67]
	Limonene	*Anabaena* sp. PCC 7120	114 µg/l	86.4 µg/l/OD_{700}/day	[68]
	Farnesene	*Anabaena* sp. PCC 7120	305 µg/l	69.1 µg/l/OD_{700}/day	[78]

Isoprenoid biosynthesis

Metabolic pathways for isoprenoid precursors

Isoprenoids and terpenoids make up a wide array of molecules that have shown promise as biofuels and their precursors. These secondary metabolites can be produced through two evolutionarily distinct metabolic pathways. These pathways are known as the mevalonate (MVA) pathway and the 2C-methyl-D-erythritol 4-phosphate (MEP; or 1-deoxy-D-xylulose 5-phosphate (DOXP); or non-mevalonate) pathway (Figure 1). The MVA route is found in eukaryotes, archaea, and some eubacteria. The MEP genes are found in plant and algal chloroplasts and most eubacteria. These categorisations of where the pathways are found can only be considered general guidelines. Lateral gene transfer has played a significant role in the genes used to produce isoprenoids.[79]

While both pathways have seven core enzymatic steps and result in the production of isopentenyl pyrophosphate (IPP) and dimethylallyl pyrophosphate (DMAPP), the pathways' precursors differ. The MEP route uses pyruvate and glyceraldehyde-3-phosphate (G3P) and, the MVA route begins with acetyl-CoA. Following the MEP route, pyruvate and G3P generate DOXP and release one CO_2 molecule via the DOXP synthase. DOXP is then taken to MEP by DOXP reductoisomerase (DXR). This DXR mediated reaction is NADPH dependent. A cytidylyltransferase then adds a cytidine phosphate group (from cytidine triphosphate - CTP) to MEP, forming 4-diphosphocytidyl-2-C-methylerythritol (CDP-ME) and releasing a free pyrophosphate. A CDP-ME kinase then adds a phophate group (from adenosine triphosphate - ATP) to form 4-diphosphocytidyl-2-C-methyl-D-erythritol 2-phosphate (CDP-MEP) and a free adenosine diphophate. CDP-MEP is then cyclised to 2-C-methyl-D-erythritol 2,4-cyclopyrophosphate (MEcPP) by MEcPP synthase, releasing a cytidine monophosphate (CMP) molecule. Using two oxidised ferredoxin units, (E)-4-hydroxy-3-methyl-but-2-enyl pyrophosphate (HMB-PP) synthase then catalyses the reaction of MEcPP into HMB-PP. The final step in the MEP pathway takes HMB-PP to IPP or DMAPP via the NADPH dependent HMB-PP reductase.

Following the MVA route, two acetyl-CoA molecules are combined with a thiolase enzyme, forming acetoactyl-CoA. The next reaction forms 3-hydroxy-3-methylgluaryl-CoA (HMG-CoA) via HMG-CoA synthase. HMG-CoA is then taken to mevalonate by the NADPH-dependent HMG-CoA reductase. Two successive ATP-dependent phosphorylations then occur, taking mevalonate to mevalonate-5-phosphate and then mevalonate-5-pyrophosphate. These reactions are mediated by mevalonate kinase and phosphomevalonate kinase, respectively. Mevalonate-5-pyrophosphate (MPP) then undergoes an ATP-dependent enzymatic decarboxylation, by MPP decarboxylase, to IPP. A bidirectional isomerase may then interconvert IPP and DMAPP.

Further enzymatic steps may take IPP/DMAPP to longer chain isoprenoid pyrophosphates. All of these elongated pyrophosphates are composed of multiple isoprene (IPP/DMAPP) units combined in a chain. IPP and DMAPP combined by a farnesyl pyrophosphate synthase (FPPS) result in geranyl pyrophosphate (GPP). FPPS can then add a second IPP molecule to GPP to result in farnesyl pyrophosphate (FPP). A third IPP molecule may then be added to FPP by a geranylgeranyl pyrophosphate synthase (GGPPS) to form GGPP. These pyrophosphates are used as the building blocks for all isoprenoids, including carotenoids and chlorophyll precursors. The MVA route is commonly referenced in engineering studies as being composed of two blocks: a "top" or "upper" mevalonate pathway composed of the first three enzymatic steps, and a "bottom" or "lower" mevalonate pathway composed of the remaining steps.[6]

Isoprenoid diversity

Tens of thousands of natural isoprenoid molecules have been described.[80] The chemical basis for all of this molecular diversity is IPP and DMAP (isoprene units), although extensive modification can be carried out on the base isoprenoid molecule. Isoprenoids can range from simple undecorated chains of isoprene units to heavily modified multi-cyclic structures that bear little resemblance to the starting precursors.

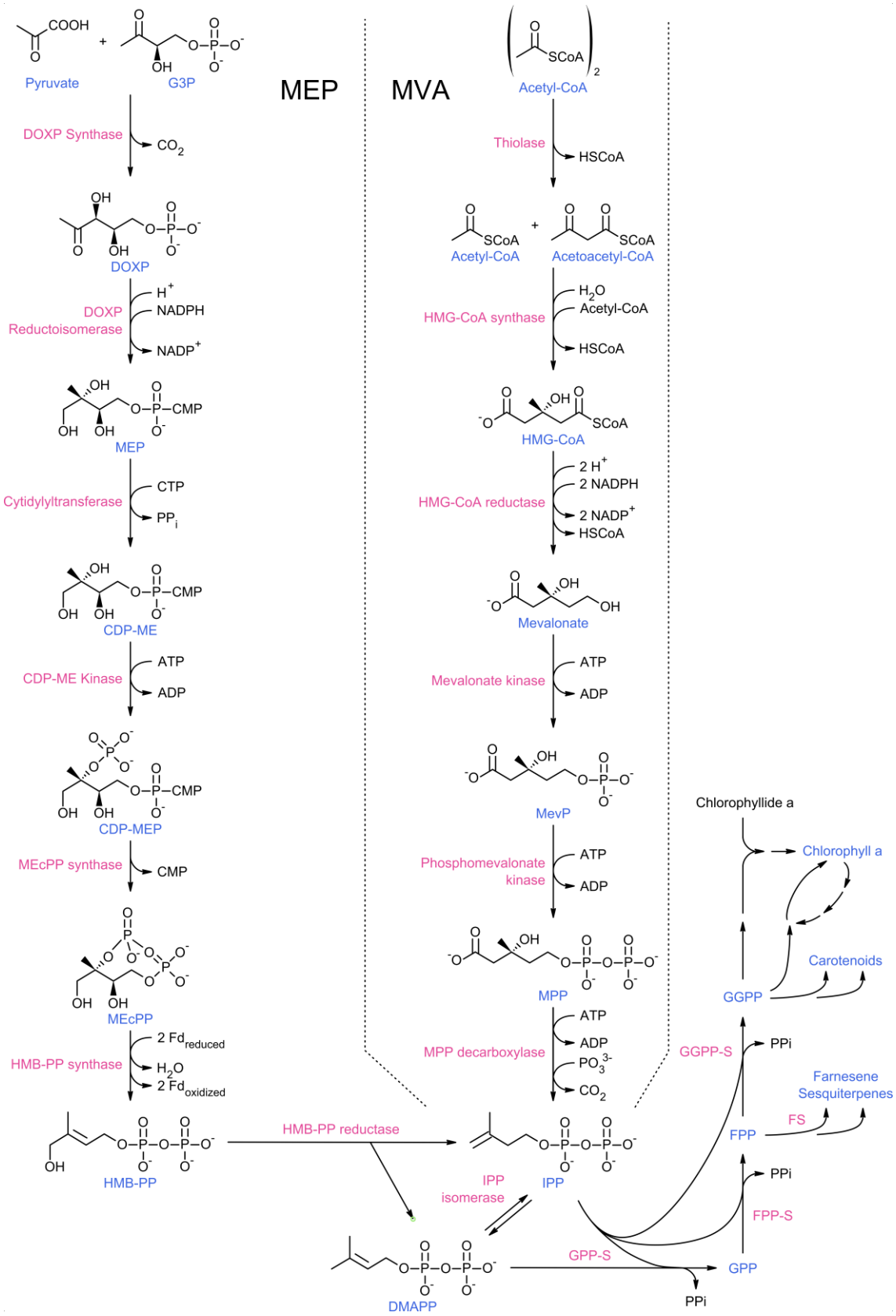

Figure 1. General isoprenoid biosynthesis routes.

2C-methyl-D-erythritol 4-phosphate (MEP) and mevalonate (MVA) isoprenoid biosynthesis routes with relevant products shown. **Abbreviations**: G3P, glyceraldehyde 3-phosphate; DOXP, 1-deoxy-D-xylulose 5-phosphate; MEP, 2C-methyl-D-erythritol 4-phosphate; CDP-ME, 4-diphosphocytidyl-2-C-methylerythritol; CDP-MEP, 4-diphosphocytidyl-2-C-methyl-D-erythritol 2-phosphate; MEcPP, 2-C-methyl-D-erythritol 2,4-cyclopyrophosphate; HMB-PP, (E)-4-hydroxy-3-methyl-but-2-enyl pyrophosphate; FD, ferredoxin; IPP, isopentyl pyrophosphate; DMAP, dimethylallyl pyrophosphate; HMG-CoA, 3-hydroxy-3-methylgluaryl-CoA; MevP, mevalonate-5-phosphate; MPP, mevalonate-5-pyrophosphate; GPP, geranyl pyrophosphate; FPP, farnesyl pyrophosphate; GGPP, geranylgeranyl pyrophosphate; '__'PP-S, '__' pyrophoshate synthase; FS, farnesene synthase.

The number of these isoprene units incorporated into the final molecule help provide a general naming system for the compounds. (Table 2) Hemiterpenes (ie. isoprene), containing only five carbon atoms, are highly volatile and have combustion properties similar to components of blended jet fuel.[81] Because of its simplicity and ease of purification, isoprene can readily be used as a chemical feedstock for producing synthetic rubber and other compounds typically generated from petroleum. Monoterpenes (with 10 carbon atoms,) such as limonene and pinene, have higher boiling points that make them suitable for use in both everyday products and high performance fuels. (Dimerised pinene has been demonstrated to have characteristics nearly identical to JP-10 tactical fuel. Petroleum based production of JP-10 is generally regarded as prohibitively expensive for general use).[82,83] Hydrogenated sesquiterpenes (with 15 carbon atoms,) such as farnesane, behave similarly to petroleum diesel during combustion. Similar to isoprene and pinene, sesquiterpenes have value as building blocks for larger molecules in chemical synthesis processes.[84–86]

Table 2. Categories of isoprenoids

Isoprenoid category	Number of carbons	Number of isoprene units	Examples and Uses (*denotes fuel use)
Hemi-terpene	5	1	*Isoprene (Platform chemical)
Mono-terpene	10	2	*Limonene (Cleaning products) *Pinene (Perfumery)
Sesqui-terpene	15	3	*Farnesene (Platform chemical) Humulene (Medical) CoQ (Health supplements) Bacteriochlorophyll precursor
Di-terpene	20	4	Retinal Taxadiene Bacteriochlorophyll precursor Chlorophyll precursor (phytol)
Sester-terpene	25	5	(*Comparatively rare in nature*)
Tri-terpene	30	6	Squalene (Cosmetics) Steroid precursor
Sesquar-terpene	35	7	(*Primarily microbial*)
Tetra-terpene	40	8	Carotenoids (Health supplements)
Poly-terpene	>40	>8	Natural rubber

Metabolic engineering of isoprenoids in cyanobacteria

Work carried out for the metabolic engineering of these isoprenoids has typically involved increasing metabolic flux through to IPP/DMAP. In eukaryotes harbouring the MVA pathway, this has been accomplished through over-expression of MVA genes or expression of a heterologous MEP pathway. Work in prokaryotes has involved the opposite: over-expression of MEP genes or expression of a heterologous MVA pathway.[87]

Over-expression of existing enzymes can be a useful tool in metabolic engineering. Such systems have traditionally been easier to construct because of the ability to PCR the relevant genes directly from the target organism. A serious drawback to relying on the organism's existing metabolism is the set of constraints imposed on any engineering designs by the cell's existing regulatory mechanisms. These mechanisms include transcriptional or translational effects, and direct regulation of the relevant enzymes. Changes induced by these mechanisms can include concentration dependent negative regulation and redirection of carbon flux to unwanted products. Using heterologous genes/enzymes can help reduce or eliminate problems associated with a cell's endogenous regulatory mechanisms.

Early (and some more recent) metabolic engineering work for isoprenoids often utilised the coloured carotenoid tetraterpenes as a screen of metabolic flux through the MEP/MVA pathway.[88–93] Carotenoids, (with the particular exceptions of phytoene and phytofluene which absorb in the ultraviolet,) range in colour from pale yellow to deep red. Including heterologous genes leading to a particular carotenoid allows for a quantifiable colourmetric assay of MEP/MVA pathway output. This type of assay is most functional in cell types with low levels of similarly coloured pigments.

As mentioned earlier, metabolic engineering of cyanobacteria for isoprenoid production is just starting to be explored.[65,67,78] Like chloroplasts and other eubacteria, cyanobacteria use the MEP pathway to generate IPP/DMAPP.

Increasing isoprenoid biosynthesis for farnesene production in cyanobacteria

The work presented here explores the use of a heterologous MVA pathway in *Synechococcus elongatus* PCC 7942 (*S. elongatus*) for α-farnesene production. Strain design for improved use in evanescent light based photobioreactors is also considered.

S. elongatus was chosen as the photosynthetic platform for exploring industrially relevant sesquiterpene production because of the broader knowledge of its physiology and genetics compared to many other microalgae. It also has a high degree of genetic tractability compared to other systems. Reliable transformation protocols have been demonstrated, including natural and conjugation based methods and, the species has a high efficiency of spontaneous, DNA sequence-mediated genomic recombination.[94,95] Additionally, multiple genomic regions have been characterised ("neutral sites") that enable foreign DNA integration with limited effect on the host.[48,96] However, a known complication to genomic integrations in *S. elongatus* is its polyploidy. The majority of cells have four or more (up to ten) copies of its chromosome at any given time.[97]

The choice of *S. elongatus* was also made because of its size. This metabolic engineering project was designed to run concurrently with the development of novel evanescent light based photobioreactors. The evanescent field generated by waveguides in this type of reactor does not penetrate far enough for optimal use of the photosynthetic machinery in larger microbes.[36,98]

Because optimal light harvesting in these systems requires a constant monolayer of cyanobacteria along the waveguide surface, it is preferable to maintain the bacteria adsorbed to the surface while flowing only media through the reactor's dysphotic/aphotic zones. To facilitate this monolayer, I attempted to reproduce a recently described knockout-induced biofilm phenotype in *S. elongatus*.[99] The original authors describe the major cause of the phenotype as inactivation of homologues of the type II secretion/type IV pilus assembly, resulting in impaired protein secretion. This impaired secretion is hypothesised to limit the functionality of a secreted peptide that facilitates self-suppression of biofilm formation.

Materials and Methods

Metabolic engineering strategy

The MVA pathway components tested here were originally designed for use in *E. coli* to increase isoprenoid production.[6] Gene components were primarily from *S. cerevisiae*, with some exceptions (Table 3). The original version of this pathway was noted to have problems with flux balances that reduced its efficiency. These imbalances (particularly HMG-CoA accumulation) have been addressed in multiple later publications.[100–103] One of the simpler methods used to improve pathway balance was carried out by screening variants of the HMG-CoA reductase.[103] Variants included a NADH-preferring version from *Delftia acidovorans* and NADPH-preferring version from *Staphylococcus aureus*. As NADPH is the major carrier of reducing equivalents in photosynthetic cells, the *Staphylococcus aureus* HMG-CoA reductase variant was chosen to be examined here first.[48]

Table 3. Mevalonate pathway genes used in this study

Pathway	Gene symbol	Gene name	Source organism	Codon optimised?	Reference source
Upper MVA	*atoB*	Acetoacetyl-CoA thiolase	*Escherichia coli*		[6,103]
	HMGS (EG13)	HMG-CoA synthase	*Saccharomyces cerevisiae*		
	HMGR	HMG-CoA reductase	*Staphylococcus aureus*	Yes (*E. coli*)[103]	
Lower MVA	*ERG12*	Mevalonate kinase	*Saccharomyces cerevisiae*		[6]
	ERG8	Phosphomevalonate kinase	*Saccharomyces cerevisiae*		
	MVD1	Mevalonate pyrophosphate decarboxylase	*Saccharomyces cerevisiae*		
	idi	Isopentenyl pyrophosphate isomerase	*Escherichia coli*		
	ispA	Farnesyl pyrophosphate synthase	*Escherichia coli*		
Farnesene	FS	α-Farnesene synthase	*Malus* × *domestica* (apple)	Yes (*E. coli*)[104]	[104]

Suitability of these pathway components for enhancing isoprenoid production in *S. elongatus* was assessed using relevant metabolites and cell growth rates. Each component block was contained in an independent operon, under the control of a single promoter (Figure 2).

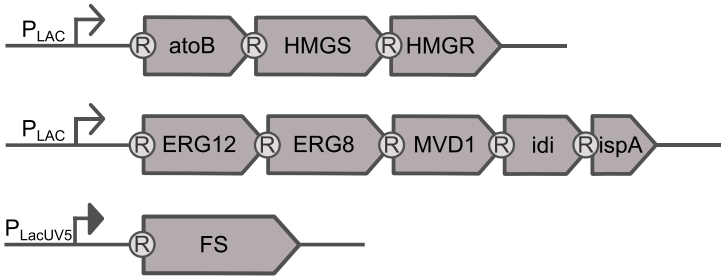

Figure 2. Heterologous operons for isoprenoid production
Genes were expressed in three separately controlled operons. The top MVA block (*atoB-HMGS-HMGR*) was under the control of a P_{LAC} promoter. The bottom MVA block (*ERG12-ERG8-MVD1-idi-ispA*) also used P_{LAC}. The farnesene synthase (FS) was under the control of a P_{LacUV5} promoter. Genes in each translational block contained separate ribosome binding sites for independent translation, indicated by ® marks. Species of origin for genes are listed in Table 3.

Functionality of the upper and lower MVA operons were assessed both independently and together. Functionality of the farnesene synthase was assessed only independently in this work. The upper pathway and farnesene synthase were assessed by end product formation (mevalonate and α-farnesene, respectively.) The lower pathway was assessed by supplying mevalonate to the culture medium.

While efficient substrate uptake is common for heterotrophic species, obligate photoautotrophs can have significantly impaired abilities to make use of fed substrates. The opposite has also been shown to occur, where synthesised small molecules remain trapped in the production host. This behaviour is linked to the loss of metabolite transporter proteins not required by photosynthetic hosts.[48]

Effects of the complete MVA pathway were examined by looking at changes to endogenous metabolism. Of particular relevance for this are the tetraterpene carotenoids, which are required for photosynthetic light capture and reduction of oxidative damage. Chlorophyll a (with its phytol {a diterpene} derived side chain,) is similarly relevant. Environmental and physiological studies also often use chlorophyll a as an additional indicator of differences in biomass.

Carotenoid levels have been demonstrated to be flexible and are typically varied by the cell to deal with changes to environmental conditions, particularly light stress. In *S. elongatus*, the major carotenoid species are β-carotene, zeaxanthin, and echinenone.[105] β-carotene is the major

species under typical laboratory conditions.[106] In this work I examine whether increased isoprenoid flux results in changes to this major isoprenoid species in *S. elongatus*. In parallel, changes to chlorophyll a content are monitored. In all instances, growth rates are recorded to assess the metabolic burden to the cell when expressing the transgenes.

All operons tested were under the control of common chemically inducible lac promoters. The upper and lower MVA operons used P_{LAC} promoters. P_{LacUV5} was used for the farnesene synthase. The lac repressor enzyme was expressed in parallel to the experimental genes, under the control of its own promoter. Lac promoters have had varying levels of efficacy in different cyanobacterial systems. In *S. elongatus*, they have seen limited, but effective use.[40,48,107–111]

Strains and media

Escherichia coli

Escherichia coli (*E. coli*) strain DH5α was used for the construction and maintenance of plasmids and, assaying of α-farnesene production. For general use, *E. coli* was grown in pre-sterilized Miller lysogeny broth (LB) at 37°C. For selection of *E. coli* on solid media, LB was mixed with 1.5% (w/v) agar. Where appropriate, antibiotics were added at the following final concentrations: ampicillin 100µg/mL, spectinomycin 50µg/mL, chloramphenicol 35µg/mL, and kanamycin 50µg/mL. For long-term storage, transformed strains were frozen at -80°C in either 7.5% dimethyl sulfoxide (DMSO) or 25% glycerol. Growth conditions for assaying of α-farnesene production were modified as listed in the GC-MS analysis section below. Culture absorbance measurements were taken in microcentrifuge tubes with a Varian Cary 50 Bio UV-Vis probe spectrophotometer.

***Synechococcus elongatus* PCC 7942**

Synechococcus elongatus PCC 7942 (*S. elongatus*) (formerly *Anacystis nidulans* R2) was the cyanobacterial species used. *S. elongatus* was grown in blue-green medium #11 (BG-11) supplemented with 20mM HEPES/NaOH pH 8.1 at 34°C.[112] For solid media, BG-11 was mixed with 1.5% (w/v) agar. Active liquid cultures were grown under 50µmol·m^{-2}s^{-1} of light and 60% humidity. Agar plates were also incubated under 50µmol·m^{-2}s^{-1} of light, except during the initial

stage of transformations. Light included in this measure was only photosynthetically active radiation (PAR) between 400 and 700nm. Light output was verified periodically with an LI-190 quantum sensor and LI-250A light meter from LI-COR Biosciences. The source used for light production was Sylvania GRO-LUX F20T12 A/WS fluorescent lamps. Non-commercial incubators used are shown in Supplementary Figure 1. For long-term storage, transformed strains were frozen at -80°C in either 7.5% dimethyl sulfoxide (DMSO) or 25% glycerol. Culture absorbance measurements were taken in microcentrifuge tubes with a Varian Cary 50 Bio UV-Vis probe spectrophotometer.

DNA handling

Oligonucleotides, synthetic double stranded fragments, laboratory DNA preparation

All oligonucleotides for PCR were purchased from Integrated DNA Technologies with 'standard desalting' as the only purification step. Lyophilised oligonucleotides were suspended in sterile double distilled water to a storage concentration of 100μM and stored at -20°C when not in use. Synthetic double stranded DNA fragments ("gBlocks Gene Fragments"), also purchased from Integrated DNA Technologies, were suspended from their lyophilised state and stored according to manufacturer instructions.

Enzymatic procedures, including restriction digestion and phosphorylation, were carried out as specified by the manufacturer. Analytical and preparative gel electrophoresis were typically carried out with 0.8% (w/v) agarose gels and standard TAE buffer, under appropriate voltage, followed by ethidium bromide based visualisation.[113]

Extraction of DNA from analytical/preparative agarose gels and clean up of enzymatic reactions were performed using spin column based kits according to manufacturer instructions (Thermo Scientific GeneJET and Qiagen). Plasmid DNA was prepared from *E. coli* cultures using spin column based 'miniprep' kits according to manufacturer instructions (Thermo Scientific GeneJET and Qiagen).

Preparation of genomic DNA from *S. elongatus* was performed using a phenol-chloroform based extraction.[46] Up to 50mL of culture was harvested by centrifugation and then suspended in

500µl 50mM Tris–HCl (pH 8.0) with 10mM EDTA, 100ul 0.6-mm-diameter glass beads, 25µL 10% sodium dodecyl sulfate, and 500uL of phenol-chloroform (1:1, v/v). Cells were then disrupted by bead homogeniser with three 2min cycles at 3000rpm, with 2min rests between cycles. The aqueous phase was separated out by centrifugation three times, with a new, equal volume of chloroform being mixed in prior to centrifugation. Genomic DNA was then precipitated with 1/10 volume 3M sodium acetate (pH 5.2) and 2.5 volumes anhydrous ethanol (-20°C) overnight. The precipitated DNA was then washed with 70% ethanol (-20°C), dried, and finally suspended in nuclease free water.

PCR for DNA part generation

High fidelity PCR for DNA part generation was carried out using Phusion High-Fidelity DNA Polymerase from Thermo Scientific or New England Biolabs. Fifty µl reactions were set up according to manufacturer instructions, including the addition of optional reaction components (1x HF buffer, 200µM dNTP mix, 0.5µM forward primer, 0.5µM reverse primer, 1ng DNA template {200ng if genomic}, 3% DMSO, 1U polymerase, nuclease free water). Standard cycling conditions were employed (typical conditions: 98°C 30sec, 30 cycles:{98°C 5sec, Primer annealing temperature +3°C 20sec, 72°C 15sec}, 72°C 5min).

PCR for screening

PCR based screening of cultures or colonies was done with ChoiceTaq DNA Polymerase (Denville Scientific). Primers used are listed in Supplementary Table 1. Fifty µl reactions were set up on ice according to manufacturer instructions (1x reaction buffer, 200µM dNTP mix, 0.5µM forward primer, 0.5µM reverse primer, cell mass as template {quantity as appropriate}, 2.5U polymerase, nuclease free water). When cells in liquid culture were required as the template, an aliquot of the culture was pelleted by centrifugation, washed with ddH_20, and pelleted again. Standard cycling conditions were employed (94°C 2min, 30 cycles:{94°C 45sec, 60°C 30sec, 72°C 1-2min}, 72°C 10min).

Strain engineering

Plasmids and strains

Plasmids and strains used in this study are listed in Table 4. *S. elongatus* transformants were generated by tri-parental mating as described in the following section. Natural transformation was also used, but found to be typically unreliable. *E. coli* transformants used to generate or maintain plasmids were generated using chemically competent cells.[114] Plasmids made in this study were generated by directional restriction cloning and non-directional restriction cloning, unless otherwise indicated. DNA parts used in assemblies were generated from existing plasmids, PCR products (including multi-template SOEing[115] products), and synthetic DNA fragments. Experimental plasmids were constructed with backbones derived from integrative shuttle vectors (pAM1573, pAM1579) from Susan Golden's laboratory at UC San Diego, modified versions of these vectors (pHN1_lacUV5) from Pamela Silver's laboratory at Harvard Medical School and, GeneArt's pSyn series shuttle vectors.[48,116,117] Knockout vectors were generated with backbone components from pTrc99a.[118]

Tri-parental mating for transformation of S. elongatus

Mating agar plates were prepared in 50mm diameter petri dishes with BG-11 agar supplemented with 5% (v/v) LB broth. Mating agar plates were then overlaid with sterile nitrocellulose disks. Alternatively, 250mm square plates can be used with multiple nitrocellulose disks per plate. One ml of *S. elongatus* culture ($Abs_{750nm} \approx 1$) was mixed with 100µl of an overnight culture of *E. coli* transformed with pRL443 and 100µls of an overnight culture of *E. coli* transformed with the *S. elongatus* shuttle vector of interest. Three plates were used for each transformation mixture: 10µl, 100µl, and the remainder of the mixture concentrated by centrifugation were spread on the nitrocellulose disks in the mating agar plates. The plates were then transferred to an incubator for 24-48 hours, cell side up, at a reduced ($30\mu mol \cdot m^{-2}s^{-1}$) light intensity. Reduced light intensity was achieved with cheesecloth or similar material. The nitrocellulose disk was then transferred with sterile tweezers to a new petri dish with BG-11 agar supplemented with the appropriate antibiotic. The selective plates were transferred to an incubator, cell side up, with full light intensity. False positives die under the selective conditions,

leaving behind putative transformant colonies. Colonies were then picking into 24-well plates containing selective BG-11 and grown under standard conditions. Antibiotic concentrations used for solid media: spectinomycin 20µg/ml, chloramphenicol 25µg/ml, and kanamycin 15µg/ml. Antibiotic concentrations for maintenance of liquid cultures were as follows: spectinomycin 10µg/ml, chloramphenicol 10µg/ml, and kanamycin 10µg/ml. Concentrations were varied from those listed when multiple selection markers were present in a strain.

Natural transformation of S. elongatus

The following protocol is as described in the literature and updated from personal communications. [96,119,120] *Synechococcus elongatus* PCC 7942 is grown to an Abs_{750nm} of 0.7. Approximately 15ml of culture is harvested by centrifugation for 10 minutes at 6000×g. The pellet is suspended in 1.5ml of sterile 10mM sodium chloride, transferred to a microcentrifuge tube, and harvested by centrifugation for 10 minutes at 6000×g. The pellet is then re-suspended in 300µl of BG-11. Fifty ng - 2µg of the DNA for transformation is added to the concentrated culture. Tubes are wrapped in aluminum foil and incubated shaking overnight at 30°C. Tubes are transferred to a shaking light incubator for four hours. Cells are spread (30µl and 270µl) onto pre-warmed BG-11 Nobel agar plates containing the appropriate antibiotic. Plates are incubated until colonies appear (1 to 2 weeks.)

Table 4. Plasmids and strains in this study

Plasmid	Description (*S. elongatus* integration cassette contents)	Reference
pSyn_2/Control	*Synechococcus-E. coli* NS1 shuttle vector, 2012 version, SpR (NS1a-SpR-NS1b)	GeneArt (ThermoFisher)
pAM1573	*Synechococcus-E. coli* NS2 shuttle vector, AmpR and CmR (NS2a-CmR-NS2b)	[116]
pHN1_lacUV5	*Synechococcus-E. coli* NS3 shuttle vector, CmR (NS3a-P_{LacUV5}-CmR-lacI-NS3b)	[48]
pTrc99a	Contains lacIq cassette, AmpR	[118]
pMTSa	Contains top MVA pathway operon: P_{LAC}MTSa, CmR	[103]
pMBIS	Contains bottom MVA pathway operon: P_{LAC}MBIS, TetR	[6]
pRL443	Conjugal plasmid for tri-parental mating, AmpR TetR KmR	[121]
pZW-(NS1:MevTSa)	pSyn2_control-version1.0_2012 derivative (NS1a-SpR-P_{LAC}MTSa-rrnB-NS1b)	This study
pZW-(NS2:MCSe)	pAM1573 derivative, enhanced multiple cloning site (NS2a-*MCSe*-rrnB-CmR-NS2b)	This study
pZW-(NS2:lacIq)	pAM1573 shuttle vector derivative (NS2a-lacIq-rrnB-CmR-NS2b)	This study
pZW-(NS2:lacIq.MBIS)	*Synechococcus-E. coli* NS2 shuttle vector, AmpR and CmR (NS2a- lacIq-P_{LAC}MBIS-rrnB-CmR-NS2b)	This study
pZW-psbA2aFS	pUC57_simple derivative, P_{psbA2}-FS-T_{BBa_B1002} , AmpR Synthesized by GenScript	[104,122] & this study
pZW-(NS3:lacI.FS)	pHN1_lacUV5 derivative (NS3a- P_{LacUV5}FS-CmR-lacI-NS3b)	This study
pZW-(2069-71:KmR)	Knockout plasmid for *Synechococcus*, pTrc99a derivative, KmR (2069frag-KmR-2071frag) for targeted knockout of Synpcc7942_2069, 2070, 2071 genes	[99] & this study

Strain	Description	Reference
Escherichia coli DH5α	*fhuA2 Δ(argF-lacZ)U169 phoA glnV44 Φ80 Δ(lacZ)M15 gyrA96 recA1 relA1 endA1 thi-1 hsdR17*	ThermoFisher
Synechococcus elongatus PCC 7942 (*Anacystis nidulans* R2)	Wild type	[123]
ZW-(NS1:MevTSa-NS2:lacIq)	*S. elongatus* strain, (NS1a-SpR-P_{LAC}MTSa-rrnB-NS1b ; NS2a-lacIq-rrnB-CmR-NS2b)	This study
ZW-(NS2:lacIq)	*S. elongatus* strain, (NS2a-lacIq-rrnB-CmR-NS2b)	This study
ZW-(NS2:lacIq.MBIS)	*S. elongatus* strain, (NS2a- lacIq-P_{LAC}MBIS-rrnB-CmR-NS2b)	This study
ZW-(NS1:MevTSa-NS2:lacIq.MBIS)	*S. elongatus* strain, (NS1a-SpR-P_{LAC}MTSa-rrnB-NS1b ; NS2a- lacIq-P_{LAC}MBIS-rrnB-CmR-NS2b)	This study
ZW-(2069-71:KmR)	*S. elongatus* strain; Knockout of Synpcc7942_2069 (partial), 2070 (full), 2071 (partial); KmR *Δ(2144977-2147246):KmR*	[99] & this study

Abbreviations: SpR - spectinomycin resistance cassette, AmpR - ampicillin resistance cassette, CmR - chloramphenicol resistance cassette, TetR - tetracycline resistance cassette, KmR - kanamycin resistance cassette, NS# - *S. elongatus* neutral integration site (genomic homology region), *lacI*/*lacIq* - lac repressor
Note 1: Current pSyn plasmids (version 2.0, 2013 release) offered by GeneArt differ from their original release (version 1.0, 2012 release.)
Note 2: The previously unavailable sequence for *HMGR*-Sa from pMTSa provided in Appendix: 'Codon optimised *HMGR-Sa* sequence'.

Analytical methods

GC-MS analysis

Mevalonate was analysed by conversion to mevalonolactone. Five hundred and sixty µl of culture was added to 140µl of 500mM hydrochloric acid and vortexed. Seven hundred µl of ethyl acetate was added to the mixture, followed by vortexing immediately for 5 minutes. The ethyl acetate phase was then transferred to an autosampler vial for analysis. Gas chromatography analysis was carried out with an Agilent 6890N gas chromatograph, 7683B injector, 5975C mass spectrometer, and Agilent DB-5MS (25m×0.2mm, 0.33µm film thickness) column. Oven program was as follows: Initial 60°C for 2 minutes, increased to 125°C at 60°C/minute, increased to 140°C at 5°C/minute, increased to 300°C at 80°C/minute, and hold at 300°C for 3 minutes. Samples were injected in 2µl volumes in pulsed-splitless mode. The injection inlet was maintained at 200°C. Hydrogen carrier gas was used, maintaining a purge flow of 60ml/minute and flow of 20ml/minute. Samples exiting the oven passed through a 240°C MSD transfer line, and onto the MS source at 230°C, MS quad at 150°C. Data was recorded at the detector following a 3.7 minute solvent delay, with *m/z* 43, 58, and 71 monitored as representative ion masses. Standard curves for DL-mevalonolactone were prepared as shown in Figure 3A-B. Mevalonate feeding was carried out with DL-mevalonate converted from 1 volume 2M DL-mevalonolactone with 1.02 volumes 2M KOH.[6]

Strains containing genes for farnesene synthesis were grown as 5ml cultures in 2YT medium with a 1ml decane overlay at 34°C. Volumes for analysis were taken directly from the decane overlay. Gas chromatography analysis was carried out with an Agilent 6890N gas chromatograph, 7683B injector, 5975C mass spectrometer, and Agilent DB-5MS column. Oven temperatures were as follows: 60°C for 2 minutes, increased to 160°C at 50°C/minute, increased to 170°C at 3°C/minute, increased to 300°C at 50°C/minute, 300°C for 3 minutes. Two µl of samples were injected with an inlet temperature of 250°C, purge flow 60ml/minute, flow 20ml/minute, pulsed-splitless mode injection, hydrogen carrier gas, 240°C MSD transfer line, 230°C MS source, 150°C MS quad, and 3.7 minute detector solvent delay. Representative ion masses monitored were 105, 161, 204 m/z. A standard curve for farnesene was prepared using an isomeric mixture as shown in Figure 3D-E.

Chlorophyll quantification

One ml aliquots of culture were taken and centrifuged to pellet in amber microcentrifuge tubes. The supernatant was discarded and 1ml of 100% methanol was added. Tubes were then vortexed for 10 minutes in the dark for pigment extraction. Cultures were again pelleted to remove cell debris. Chlorophyll determination was carried out by absorbance recordings at 663nm in a 1cm cuvette.[43,124]

HPLC analysis of carotenoids

Sample extraction was carried out in the same manner as for chlorophyll quantification. Methanol extracts were transferred to amber autosampler vials for analysis. Carotenoids were separated by HPLC on a Agilent Zorbax Eclipse XDB-C18 column (3.5µm, 150×4.6mm) using a 15 minute gradient of ethyl acetate (0-100%) in an acetonitrile-water-triethylamine solution (9:1:0.01, vol:vol:vol) at 1.5ml/minute.[43] β-carotene was identified by its typical retention time and appropriate analytical standard. A standard curve for β-carotene was prepared as shown in Figure 3C.

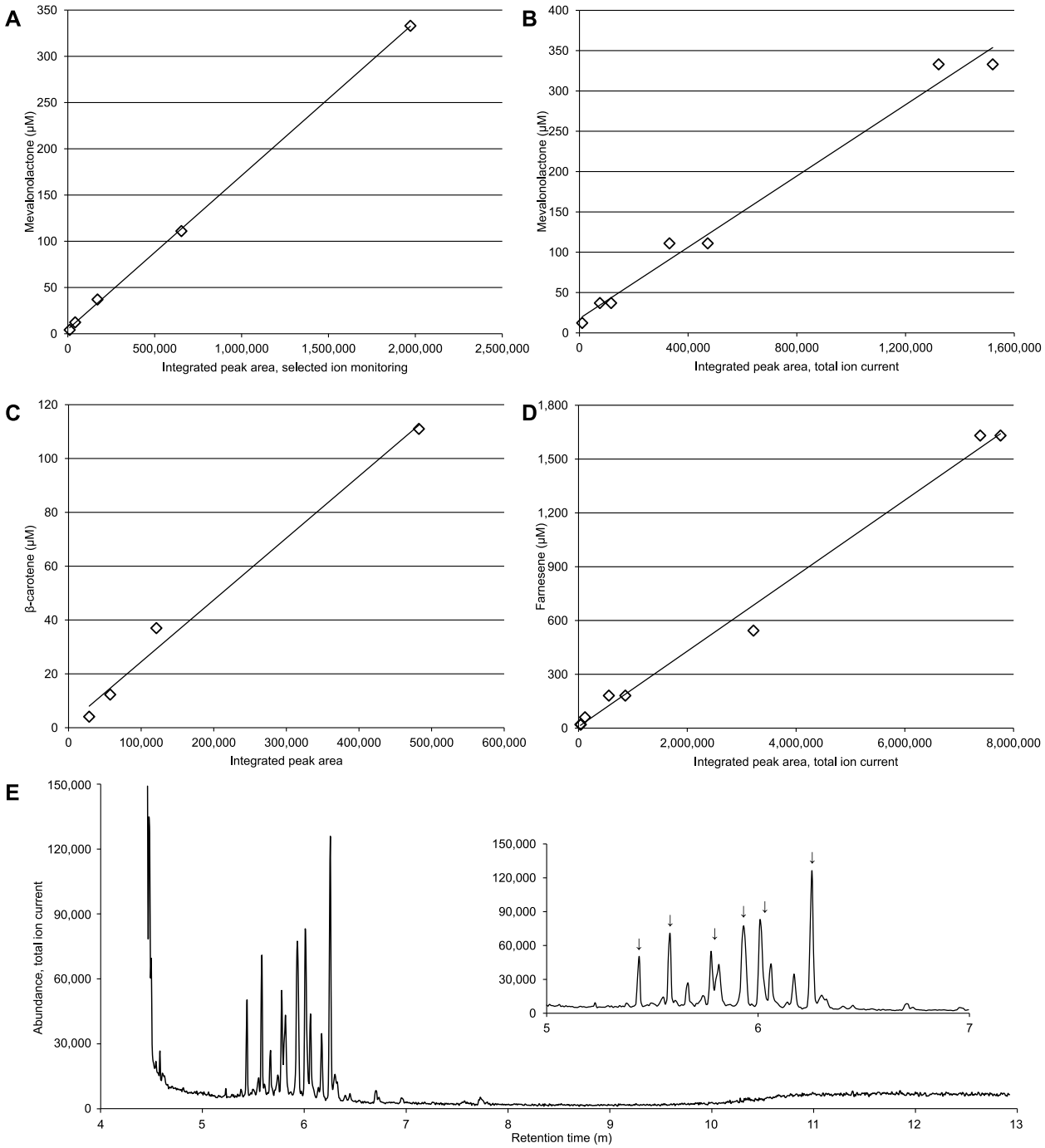

Figure 3. Standard curves used for quantitative analysis of metabolites

(A) DL-Mevalonolactone standard curve for GC-MS analysis using selected ion monitoring data. (B) DL-Mevalonolactone standard curve for GC-MS analysis using total ion count data. (C) β-carotene standard curve for HPLC analysis. (D) Farnesene (isomeric mixture) standard curve for GC-MS analysis using total ion count data. (E) GC chromatogram of farnesene (isomeric mixture) used to generate the standard curve shown in D. Insert shows magnified section of chromatogram, with arrows indicating major farnesene isomer peaks.

(A) Eq. 1: Mevalonolactone 1 standard curve fit

$y = (0.0002x + 4.47416) \times 0.118 \times (6/0.7)$; $R^2 = 0.9996$

(B) Eq. 2: Mevalonolactone 2 standard curve fit

$y = (0.0002x + 17.726) \times 0.118$; $R^2 = 0.9859$

(C) Eq. 3: β-carotene standard curve fit

$y = (0.0002x + 1.491)$; $R^2 = 0.9884$

(D) Eq. 4: Farnesene isomers standard curve fit

$y = (0.0002x + 8.2254)$; $R^2 = 0.9916$

Results

Transformations of S. elongatus

Both natural transformations and tri-parental mating were employed as methods to obtain transformed *S. elongatus* strains. Use of natural transformation has been reported extensively in the literature but was not a reliable method of transforming *S. elongatus* in my hands. Natural transformation positive controls generally resulted in dense lawns. With this method, colony forming units were not reliably countable; even with serial dilutions plates tended to have diffuse growth rather than punctiform/circular colonies. Experimental conditions varied for this method included antibiotic concentration, starting culture density, incubation time, recovery time, and plasmid concentration. Based on these results, tri-parental mating was tested for as an alternative method for transforming DNA into *S. elongates.* No experimental strains discussed in the following sections were generated by the natural transformation method.

Tri-parental mating for transformation of *S. elongatus* is uncommon in the literature due to increased complexity and cost. The nitrocellulose disk used with the mating method provided improved anchorage for colonies and recorded conjugation efficiencies were up to 8×10^{-2} colonies/CFU. Positive confirmation of colonies by PCR after growth in liquid culture, as shown in the proceeding sections, was typically less than 10%.

Microbial contamination of strains was common both during and after transformation procedures, and contaminating species varied. Contaminating species were typically visible only after enrichment overnight on 2YT agar or as micro-punctiform colonies. As other species have the potential to alter the metabolic profile of a sample, contaminated samples were not included in analyses.

Validation of PCR screen for S. elongatus integration events

Following tri-parental mating and selection, successful integration of heterologous mevalonate pathway genes into *S. elongatus* was initially verified by PCR screening carried out directly on pelleted cells grown from single colonies. Figure 4 shows validation of reaction

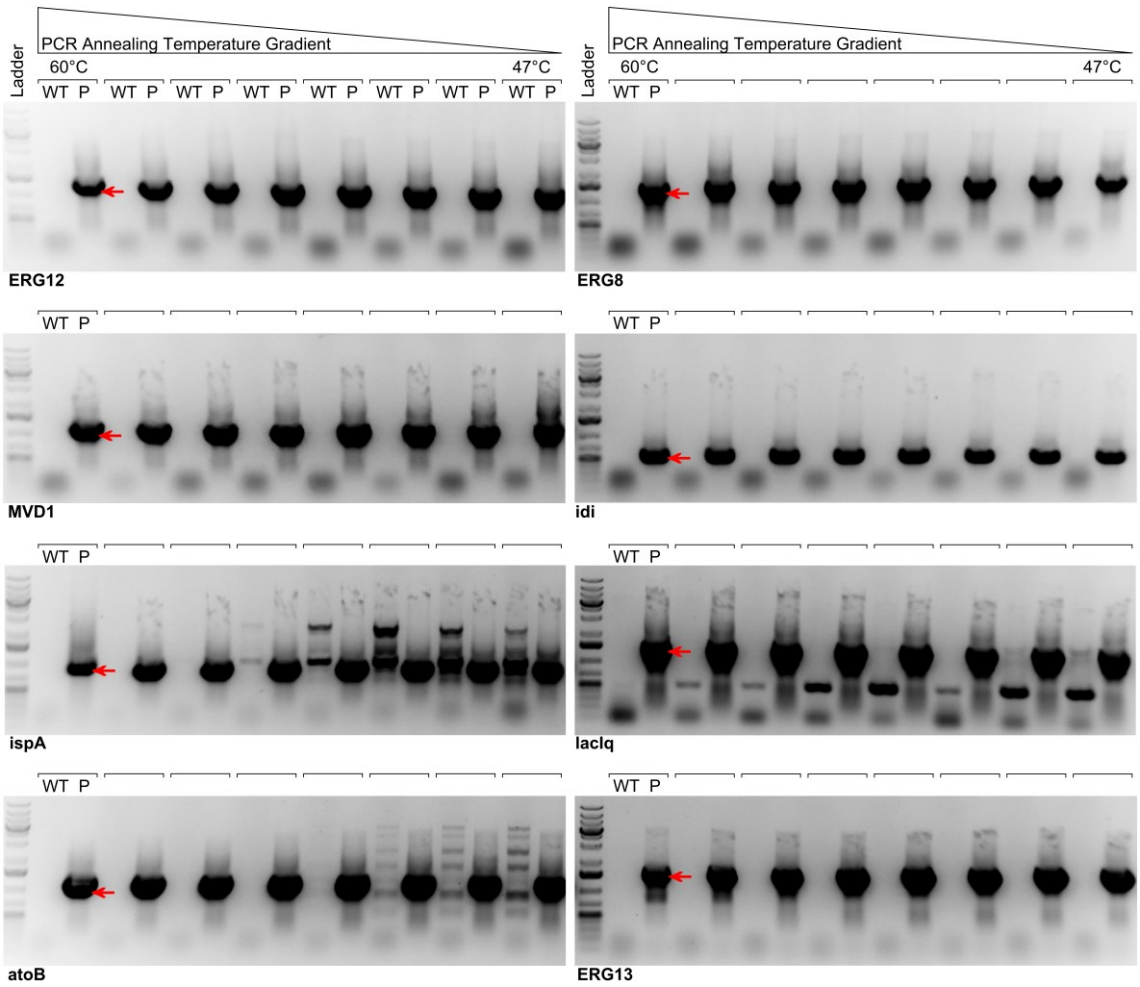

Figure 4. Validation of PCR based screen for *S. elongatus* chromosomal integration events
Two reactions are carried out at each temperature in the gradient. The negative control 'WT' reaction uses wild type *S. elongatus* cell mass used as the PCR template. The 'P' reaction uses a gene specific plasmid. *ERG12*, *ERG8*, *MVD1*, *idi*, *ispA*, *lacIq* use pZW-(NS2:lacIq.MBIS). *atoB* and *ERG13* use pMTSa. Ladder is Generuler 1kb+ by ThermoFisher. Bottom bands in lanes without ladder are primer dimers.

specificities for the PCR screening used on putative transformants. Nine target sequences were validated for their viability in screening. Template DNA used for validation was 1) a plasmid containing the mevalonate pathway and related genes (positive control) and, 2) wild type *S. elongatus* pelleted cells (negative control). PCR conditions, except annealing temperature, were consistent for all reactions. At the highest annealing temperature used (60°C), no significant non-specific bands appeared in the agarose gel electrophoresis analysis of the reactions, with the exception of primer dimers (Figure 4). Non-specific priming on the *S. elongatus* genome was seen in three out of eight of the primer pairs and, was greatest at lower PCR annealing

temperatures. PCR of the *HMGR*-Sa gene was unsuccessful on multiple occasions. Each instance of non-specific priming occurred where the target DNA sequence was of bacterial origin, as opposed to from *Saccharomyces cerevisiae* (Figure 2). From these screen validation results it can be concluded that when using a 60°C annealing protocol this PCR screening method is highly specific for the target DNA and false positives from genomic mispriming are unlikely.

Mevalonate biosynthesis by S. elongatus cells harboring a recombinant upper mevalonate pathway

The three-gene upper-portion of the mevalonate pathway (MevT) was stably integrated into a *S. elongatus* strain carrying the lac repressor by tri-parental mating. These three genes, *atoB*, *ERG13*, and *HMGR*-Sa, were contained in a single operon (MevT-Sa.) This operon was under the control of a standard inducible bacterial lac promoter (P_{Lac}) (Table 4).

S. elongatus colonies from the selective post-conjugation plates to be tested for positive integration of the 3-gene pathway were picked and used to inoculate BG-11 cultures. Once cultures were a pale to medium green colour, 200µl from each culture was harvested by centrifugation. Cell lysates were used as template for verification by PCR that the MevT operon was present in the cells. Screening was carried out with *atoB_fwd* and *ERG13_rev* primers, resulting in a longer DNA fragment size than seen in the method validation shown in Figure 4. As done previously, the positive control used a plasmid DNA template and the negative used wild type cell mass. Only one out of seventeen cultures screened for MevTSa integration was shown to contain the heterologous DNA (Figure 5). The PCR product generated from this strain clearly demonstrates the presence of the upper mevalonate pathway in the strain.

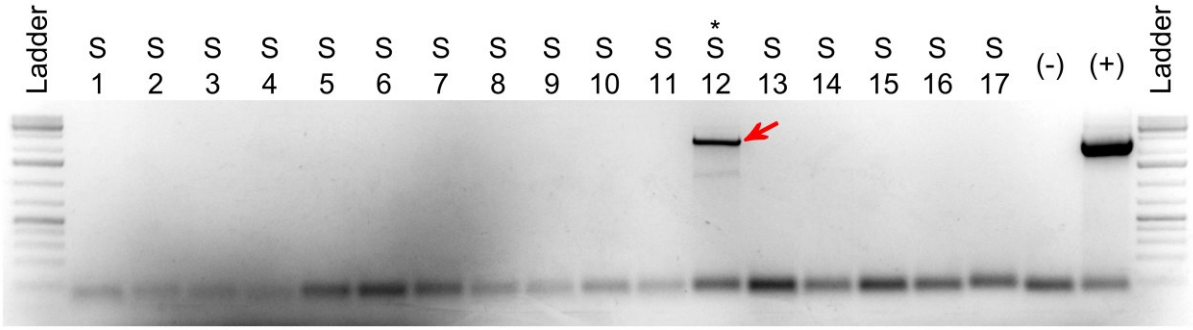

Figure 5. Verification of upper MVA pathway integration by PCR.
Ladder is Generuler 1kb+ by ThermoFisher. 'S' denotes experimental *S. elongatus* strains. Sample S12 represents the only successful integrant in this screen where the upper band matches expected *atoB-ERG13* fragment size. Negative control with wild type *S. elongatus*. Positive control with pMTSa plasmid. Bottom bands in lanes without ladder are primer dimers.

To test for functionality of the chromosomally-integrated upper mevalonate pathway in the engineered *S. elongatus*, cells were tested for the production of mevalonate. Four biological replicate cultures of *S. elongatus* containing the MevT-Sa operon were grown under maintenance conditions until log phase was reached after approximately four days. The four cultures were then diluted to 0.1 Abs_{750nm} (time 0 - t0) and split into two sets of flasks. IPTG was added to one of the sets at t0 to induce MevT operon expression. Cultures were tested for contamination by spot plating 10µl of each culture onto LB agar plates at each analysis time point. No contamination was recorded in any of the samples during this time course. At the same time a sample was taken for spot testing, additional samples were taken to monitor cell density and for mevalonate analysis.

Similar growth rates were recorded for both induced and uninduced cultures, although the statistical confidence interval (and standard deviation) for the absorbance measurements were noted to increase substantially as the time course progressed (Figure 6A).

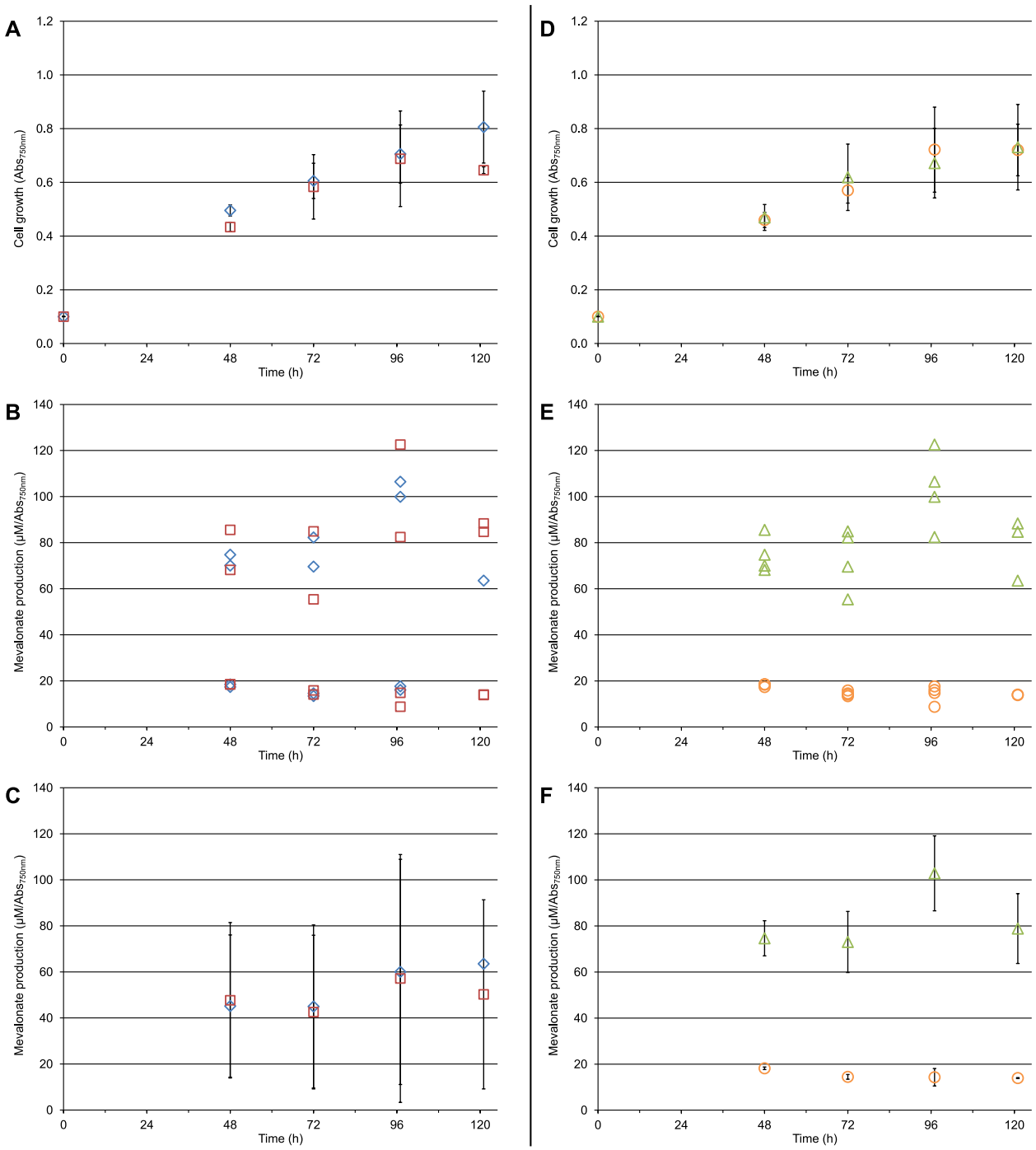

Figure 6. Mevalonate biosynthesis in a *S. elongatus* strain containing an upper MVA pathway
Mevalonate production by the ZW-(NS1:MevTSa-NS2:lacIq) *S. elongatus* strain. (A-C) show cultures without (◊) and with (□) 500μM IPTG inducer added. (A) Growth curves of the uninduced/induced strains. (B-C) GC-MS analysis of mevalonate production for the uninduced/induced strains. (D-F) show the same cultures re-plotted into non-expressing/low-mevalonate (△) and expressing/high-mevalonate (○) groups. (D) Growth curves of the regrouped strains. (E-F) GC-MS analysis of mevalonate production for the regrouped sets of strains. Mevalonate was measured indirectly following acidification of samples to form mevalonolactone. Error bars indicate the mean ± 95% confidence interval of four biological replicates.

Solvent extracted samples were analysed for mevalonate by GC-MS. Measured ion counts were converted to molar concentrations based on a standard curve and then normalized to cell density. Figure 6B shows the individual replicates for uninduced and induced cultures at each time point. Averaging these replicates (Figure 6C) results in the 95% confidence interval being approximately as large as the measurements themselves, suggesting no correlation between strain induction and mevalonate production.

Figure 6E shows the same individual data points reorganized into low and high mevalonate concentration samples. All previous data points were retained. These re-clustered data points are shown averaged together in Figure 6F. Both low and high mevalonate categories are noted to remain at approximately the same concentration, at a 95% confidence interval, between the measured time period of 48-121 hours. When re-clustered in this way, growth rates (Figure 6D) remain similar in appearance, with limited change in the mean growth rates and associated confidence intervals.

Analysis of mevalonate content in these culture extracts demonstrates that 1) mevalonate production under the control of P_{Lac} is independent of IPTG induction in this system and, 2) that two distinct populations of mevalonate producing cells were present. One population produced just under 20μM/Abs_{750nm}, while the other was approximately four times higher at 80μM/Abs_{750nm} (Figure 6E-F).

Mevalonate uptake and utilization by S. elongatus cells harbouring a lower mevalonate pathway

Conjugation based integration of the five-gene lower half of the mevalonate pathway was also screened for by PCR. Both pZW-(NS2:lacIq.MBIS) containing the lac repressor and the lower MVA pathway and, pZW-(NS2:lacIq) containing only the lac repressor were transformed. The PCR screening was performed directly on pelleted cell mass from liquid cultures of putative transformants, as described in the previous section.

The lac repressor PCR product seen from both recombinant strains clearly shows the presence of the gene in these strains (Figure 7). The presence of the *ERG12* PCR product for the lower mevalonate pathway demonstrates the presence of the operon in the NS2:lacIq.MBIS

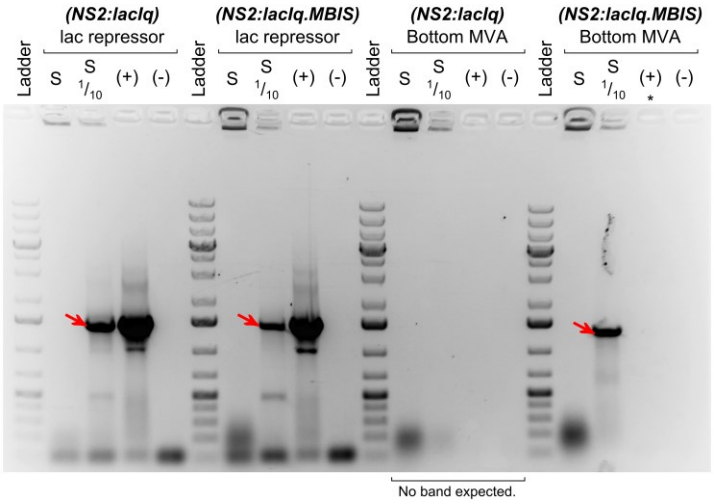

Figure 7. Verification of lower MVA pathway integration by PCR.
Ladder is Generuler 1kb+ by ThermoFisher. 'S' denotes experimental *S. elongatus* strains. '$^{1}/_{10}$' denotes dilution of cell culture template by factor of 10. Upper bands in S$^{1}/_{10}$ columns match expected product sizes. (*lacIq* used for lac repressor screen; *ERG12* used for lower MVA screen.) Negative control with wild type *S. elongatus*. Positive control with corresponding pZW-(NS2:lacIq) and pZW-(NS2:lacIq.MBIS) plasmids. Genomic DNA can be seen retained at the top of the agarose gel in S and S$^{1}/_{10}$ lanes. ' * ' denotes lane with failed positive control for lower MVA pathway.

strain. Although previously validated (Figure 4), the positive control for the lower MVA pathway PCR reaction failed (Figure 7).

Functional screening of the MBIS-harbouring recombinant strains was carried out by measuring mevalonate utilization. Both NS2:lacIq and NS2:lacIq.MBIS strains were grown in quadruplicate in the presence of IPTG and displayed growth rates with no significant differences at the 95% confidence interval (Figure 8A). These similar growth rates suggest no apparent metabolic burden in the strain caused by the lower MVA genes. Cultures were tested for contamination by spot plating 10µl of each culture onto LB agar plates at each analysis time point. No contamination was recorded in any of the samples during this time course. No change in mevalonate concentration, which would point to a functional lower mevalonate pathway, is seen in either the experimental NS2:lacIq.MBIS strain or NS2:lacIq control strain (Figure 8B). This lack of utilization of mevalonate by the lower MVA strain suggests either pathway inactivity or limited intracellular substrate availability.

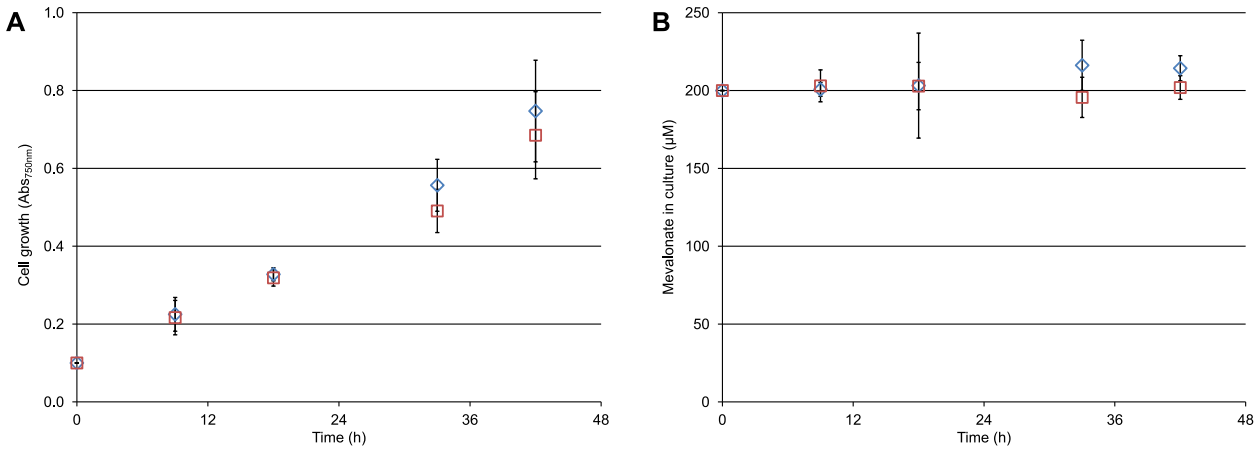

Figure 8. Mevalonate feeding in *S. elongatus* harbouring a lower MVA pathway
Metabolism of fed mevalonate by the ZW-(NS2:lacIq.MBIS) *S. elongatus* strain (□) and the control ZW-(NS2:lacIq) strain (◊). (A) Growth curves of the strains with supplemented mevalonate. (B) GC-MS analysis of the total mevalonate present in the cultures over the recorded growth period. Mevalonate was measured indirectly following acidification of samples to form mevalonolactone. Error bars indicate the mean ± 95% confidence interval of four biological replicates.

Changes to host metabolism while harbouring a complete heterologous mevalonate pathway

To test if limited intracellular substrate availability was responsible for the lack of mevalonate utilization, the upper MevT-Sa operon-(NS1:MevTSa plasmid) was integrated into NS2:lacIq.MBIS by tri-parental mating. Successful integration of both the upper and lower mevalonate pathway operons into a single strain was once again screened by PCR following selection and growth of putative transformants on the appropriate antibiotics (Figure 9). Two correct transformants were recovered out of the thirty cultures screened. One of these transformants shown in Figure 9, strain S7, was then chosen for functional screening. The presence of PCR products for both the lower ('B' lane) and upper ('T' lane) clearly demonstrates the presence of the complete heterologous pathway in the strain.

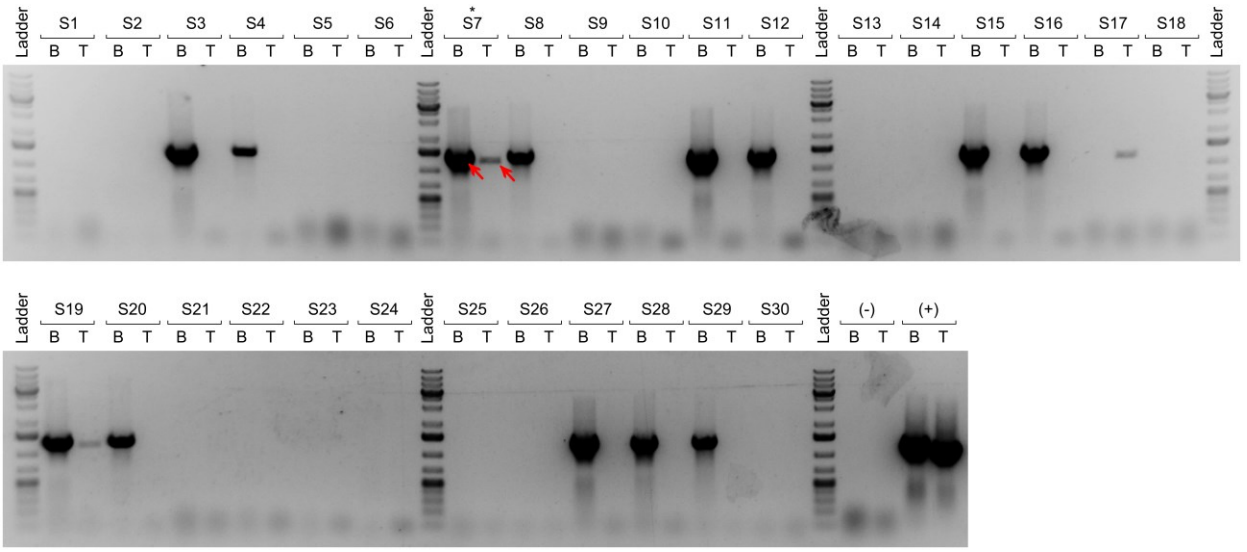

Figure 9. Verification of complete MVA pathway integration by PCR.
Ladder is Generuler 1kb+ by ThermoFisher. 'S' denotes experimental *S. elongatus* strain. 'B' denotes the lower (bottom) MVA pathway and 'T' the upper (top) MVA pathway. Bands in S columns match expected product sizes. (*ERG12* used for bottom MVA screen; *atoB* used for the top MVA screen.) Negative control with wild type *S. elongatus*. Positive control pZW-(NS2:lacIq.MBIS) plasmid for bottom MVA pathway ('B') and pMTSa for top MVA pathway ('T'). Bottom bands in lanes without ladder are primer dimers..

Chlorophyll content in the MVA containing strain

As chlorophyll a is an isoprenoid derivative and is often used to characterise algal growth, chlorophyll a content over time (Figure 10C) was characterised by bulk absorbance measurements at 663nm. The *S. elongatus* strain containing the complete heterologous mevalonate pathway was grown in parallel with wild type *S. elongatus* and chlorophyll was extracted. At a 95% confidence interval the growth rates of the recombinant and wild type strains showed no significant differences in most of the recorded time points (Figure 10A). When the confidence interval is reduced to 90%, a consistent decrease in growth rate is apparent for the double integrant stain over the first 54 hours of growth, indicating that the recombinant strain is subject to an increased metabolic burden compared to the wild type (Figure 10B). At 18 hours of growth, the total chlorophyll a was 26% higher for the wild type strain versus the experimental strain. At a 95% confidence interval there was no significant difference between total chlorophyll a content following the first time point, with the exception of hour 54. At hour 54 the experimental strain had an 8.8% higher total chlorophyll a concentration.

When chlorophyll a content is normalised to culture density, a different trend can be seen (Figure 10D). At 18 hours there is no significant difference between the wild type and the engineered strain. For the remainder of the time course, the normalised chlorophyll a concentration is 25 to 37% higher in the engineered strain. While the total chlorophyll a content trends upwards for both strains over the time course, the concentration is shown to trend downwards when normalised to culture density.

To examine the differing rates of chlorophyll and biomass accumulation, the same data set is shown normalised to the maximum value for each condition in Figure 10E-F. In wild type cells, the rate of chlorophyll accumulation is higher earlier in growth. By 18 hours, the wild type strain has accumulated 80% of its maximum chlorophyll content compared with only 60% of the maximum for the modified strain. For both strains the culture densities have reached approximately 50% of their maxima at this time point. Differences in maximum quantities for both chlorophyll and culture density are not statistically significant between the wild type and engineered strains. From these differences in chlorophyll a accumulation, we can speculate that inclusion of a complete MVA pathway has a direct effect on central metabolic processes in *S. elongatus* and the strain maintains higher concentrations of chlorophyll a after an initial lag.

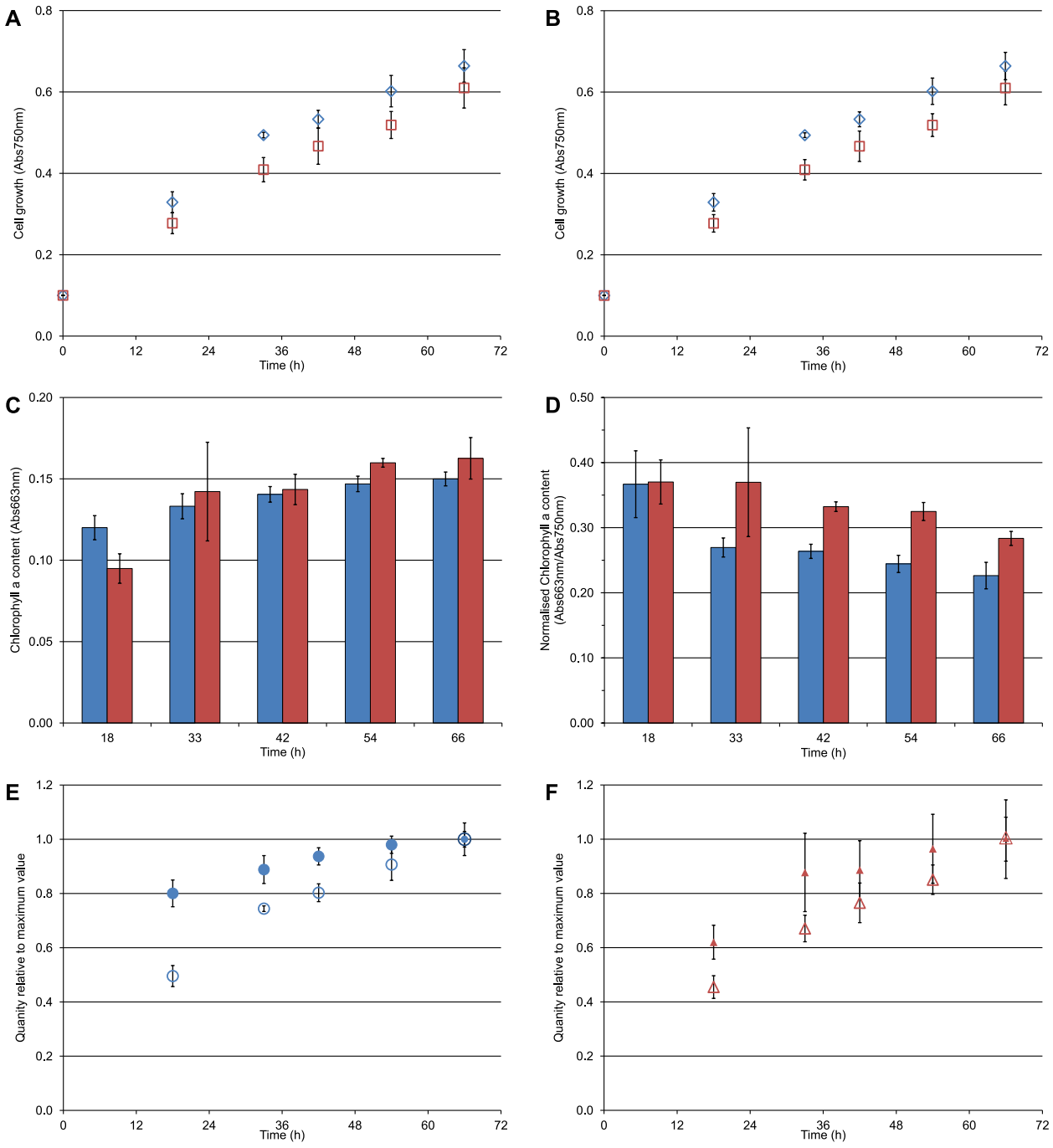

Figure 10. Chlorophyll a biosynthesis in a MVA pathway containing *S. elongatus* strain
Analysis of chlorophyll a production in a *S. elongatus* strain containing a complete heterologous mevalonate pathway. (A-D) (◊ and blue bars) show the wild type *S. elongatus* and, (□ and red bars) show the ZW-(NS1:MevTSa-NS2:lacIq.MBIS) strain. Growth curves of the strains are shown with error bars indicating the mean ± 95% confidence interval (A) and ± 90% confidence interval (B). (C) Total chlorophyll a content is compared between the strains. (D) Chlorophyll a content normalised to culture growth is compared. (E) Culture growth (○) and chlorophyll accumulation (●) normalised to their recorded maximums for the control strain. (F) Culture growth (△) and chlorophyll accumulation (▲) normalised to their recorded maximums for the heterologous mevalonate pathway strain. Culture density (750nm) and chlorophyll a content (663nm) were both measured by spectrophotometer. Error bars indicate the mean ± 95% confidence interval of the biological replicates, except as indicated for (B).

β-Carotene content

The same cultures used for chlorophyll analysis were also analyzed by HPLC for changes to β-carotene content as a general indicator of cellular isoprenoid production. The strain expressing the heterologous mevalonate pathway showed no statistically significant trend in total β-carotene levels compared to the wild type strain (Figure 11A). However, differences were apparent when β-carotene content was normalised to culture density (Figure 11B). At a 95% confidence interval, normalised β-carotene content is seen to be higher in the engineered strain up until hour 42. At a 90% confidence interval, all time points except at hour 54 show significantly higher normalised β-carotene content. From this we can conclude that the recombinant strain maintains

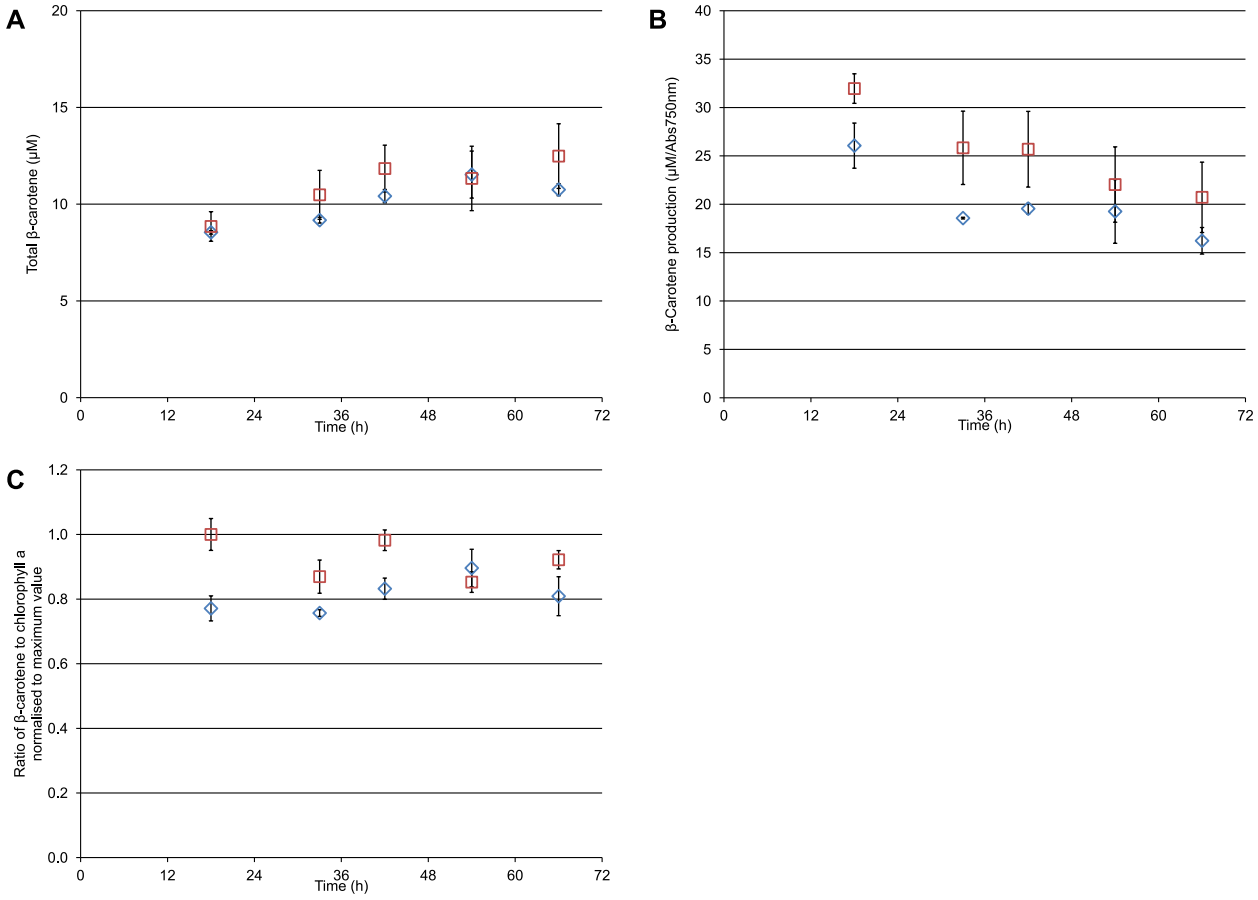

Figure 11. β-carotene biosynthesis in a MVA pathway containing *S. elongatus* strain
Analysis of β-carotene production in a *S. elongatus* strain containing a complete heterologous mevalonate pathway. (◊) show wild type *S. elongatus* and (□) show the ZW-(NS1:MevTSa-NS2:lacIq.MBIS) strain. β-carotene was measured by HPLC. (A) Total β-carotene content in the cultures. (B) β-carotene content normalised to culture growth. (C) The ratio of β-carotene to chlorophyll a shown normalised to the highest recorded ratio. Error bars indicate the mean ± 95% confidence interval of 3 (◊) or (□) 5 biological replicates.

higher concentrations of the isoprenoid β-carotene even as concentrations drop during the stationary growth phase.

In the wild type cells, the ratio of β-carotene to chlorophyll shows limited variation over the time course (Figure 11C). This contrasts with the engineered strain where, a downward trend in the β-carotene:chlorophyll ratio is apparent, similar to that seen in the β-carotene:Abs_{750nm} values. The ratio of β-carotene to chlorophyll shows a similar trend to that of β-carotene to culture density. From these ratios we can conclude that β-carotene is a potential sink for additional flux of isoprenoid precursors generated by the MVA pathway. This relationship is considered further in the Discussion.

Biosynthesis of α-farnesene

For a direct measurement of increased isoprenoid flux in the engineered *S. elongatus,* an α-farnesene synthase, previously codon optimised for *E. coli* by Wang *et al.*, was synthesised and expressed under the control of the native *S. elongatus psbA2* diurnal promoter. To validate the functionality of the encoded protein, the farnesene synthase was cloned into the pHN1_lacUV5 shuttle vector under the control of a lac promoter to form pZW-NS3:lacI.FS and transformed into *E. coli*. The synthase is known to produce a single isomer of farnesene, however, I was unable to obtain an analytical standard containing only α-farnesene and instead used an isomeric mix. As the multiple isomers were resolved as separate peaks during GC-MS analysis, all peaks were integrated and summed together to construct the standard curve (Figure 12A).

E. coli cultures harbouring the synthase-expressing plasmid were grown under selection at 37°C and diluted to a starting Abs_{600nm} of 0.05 (Figure 12B). Cultures were then switched to 34°C to better approximate *S. elongatus* growth conditions and overlayed with decane to trap produced farnesene. After approximately 9 hours, cultures reached an Abs_{600nm} of 0.5 and one set of the cultures had IPTG inducer added. Decane samples were taken at the time of induction as well as at 12 and 24 hours post induction. At 12 and 24 hours post-induction, culture density in the induced samples was noted to be higher. Farnesene was already detectable at the time of induction and total extracted farnesene increased only slightly over the following 24 hours. (Figure 12C-D). From these data from *E. coli* data, it was concluded that the synthase is functional in its expression system.

Integration of the synthase-expressing pZW-NS3:lacI.FS into *S. elongatus* was attempted, but was unsuccessful. PCR based screening, as described previously, was carried out on putative transformants (Figure 13).

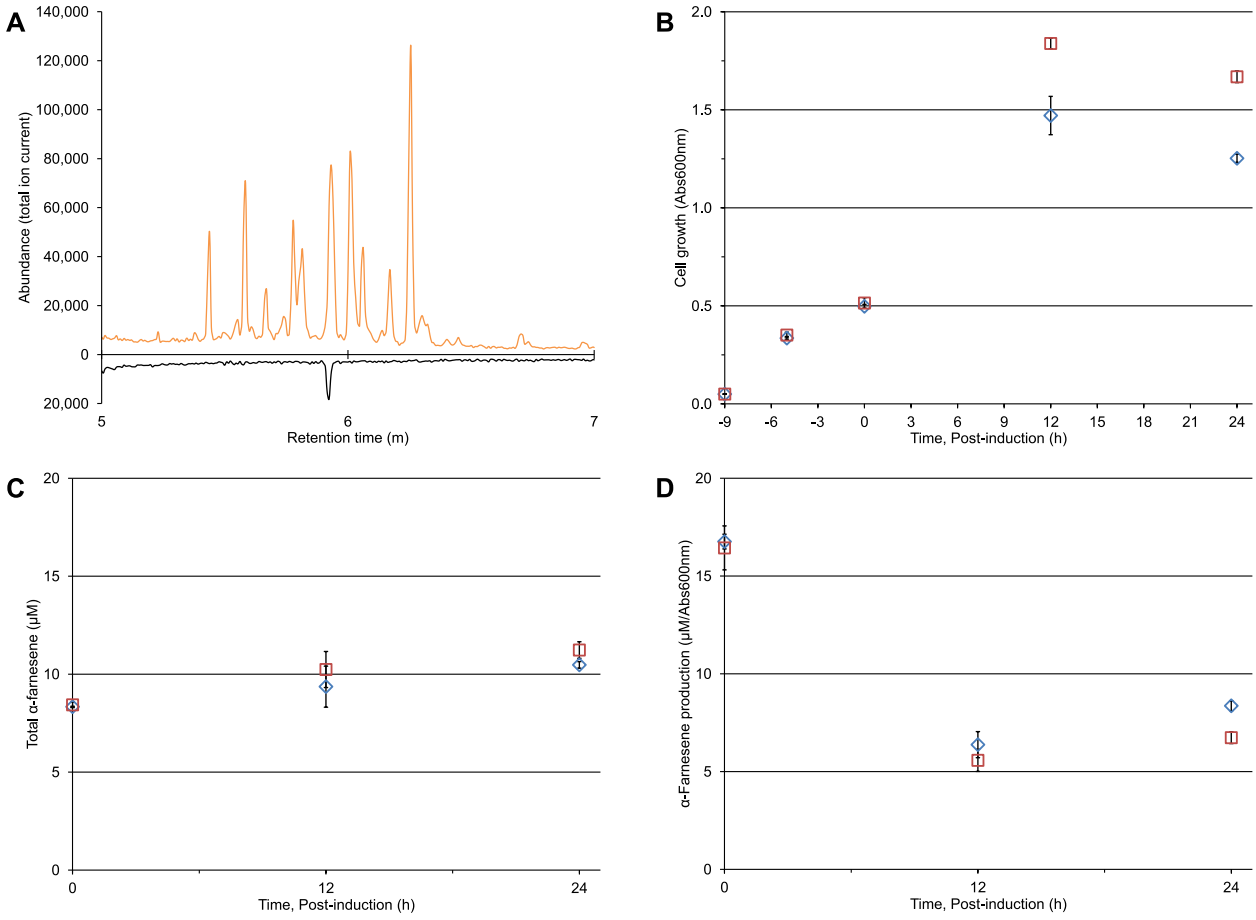

Figure 12. Functional testing of the α-farnesene synthase in a *S. elongatus* shuttle vector
Functionality of farnesene synthase in a *S. elongatus* shuttle vector determined by GC-MS. The pZW-NS3:lacI.FS plasmid was expressed in *E. coli* in a two-phase culture of 2YT medium and decane. (A) The upward y-axis shows the GC-MS chromatogram used to generate a standard curve (farnesene, isomeric mixture - 181μM). The downward y-axis shows an experimental chromatogram (α-farnesene - 11.7μM). (B-D) show cultures without (◊) and with (□) 500μM IPTG inducer added. (B) Growth curves of the cultures are shown. (C) Total α-farnesene content for the uninduced and induced cultures is shown.. (D) α-Farnesene content normalised to culture growth is compared for both conditions. Error bars indicate the mean ± 95% confidence interval of four biological replicates.

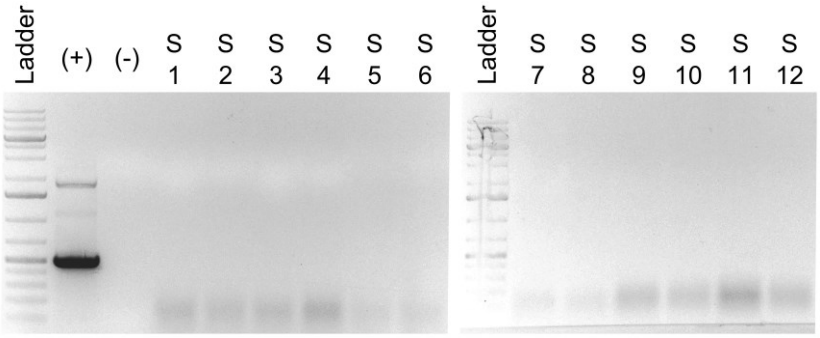

Figure 13. Screening for farnesene synthase integration by PCR.
Ladder is Generuler 1kb+ by ThermoFisher. 'S' denotes experimental *S. elongatus* strain. Positive control uses a 490bp segment (lower, higher intensity band) of the farnesene synthase from pZW-NS3:lacI.FS. Negative control with wild type *S. elongatus*. Bottom bands in lanes without ladder are primer dimers.

Genetic knockout induced biofilm formation in S. elongatus

Optimal light harvesting in evanescent-field based photobioreactors requires a constant monolayer of cyanobacteria along the waveguide surface. Use of a biofilm phenotype was hypothesised to allow consistent light and nutrient availability to such a cell monolayer in this type of photobioreactor. Currently, the only reported biofilm phenotype in *S. elongatus* was reported by Schatz *et al.* in 2013. Their strain displayed a distinct biofilm phenotype, as well as a loss of competence. The authors showed that a knockout of *S. elongatus* gene 2069 or gene 2071 was necessary and sufficient under normal conditions to generate the phenotype in wild type cells (Figure 14A). Because of the competency loss, I constructed a knockout vector - analogous to that used by Schatz *et al.* - which could be used as a final transformation with any experimental strain (Figure 14B).

Transformation by bacterial conjugation was attempted with an appropriate, broad range of kanamycin concentrations (5, 10, 15, 20, 25µg/ml) on solid media. Individual colonies were then transferred to liquid media in 24-well plates under continued selection or re-streaked and then transferred to liquid media. Over multiple rounds of conjugation, in excess of 200 colonies were screened for phenotypic changes. I was unable to reproduce the desired biofilm phenotype under any of the tested selective conditions.

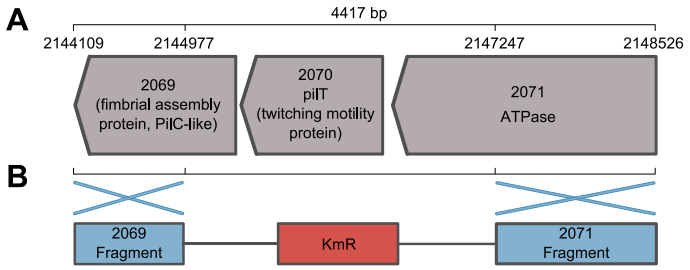

Figure 14. *S. elongatus* biofilm-related genome features
S. elongatus biofilm phenotype-associated locus. (A) Shows the genomic region containing biofilm linked genes. Each block is a native gene listed with its identification number. Genome nucleotide positions are listed above the blocks. (B) Shows the functional components of an insertional knockout plasmid. The recombination event is selected for by the kanamycin resistance cassette shown between the genomic sequence fragments. Not shown is the plasmid's pUC origin for propagation in *E. coli*.

Discussion

Photosynthetic isoprenoid production for commodity chemicals

Biosynthetic farnesene production has been demonstrated in a variety of industrial microorganisms. Production in *S. cerevisiae* is now commercially viable, with it being sold under the trade name Biofene by Amyris.[125] While I was able to demonstrate only preliminary functionality an α-farnesene production vector for use in *S. elongatus* here, similar work done in other cyanobacteria species and with different target molecules suggests the strategy proposed here is feasible (Table 1). A 2.5-fold increase in heterologous isoprenoid production in the related *Synechocystis* species when a complete MVA pathway was expressed suggests isoprenoid production can benefit in this type of host by the inclusion of the MVA pathway.[67]

Because the endogenous MEP isoprenoid pathway in *S. elongatus* is directly linked to multiple components of the photosynthetic process (i.e. chlorophyll and carotenoids) (Figure 1), balancing metabolic flux in a strain with engineered MEP over-expression may be more challenging. Engineering efforts for increasing production of heterologous isoprenoids by increasing flux through the endogenous MEP pathway have focused on pushing more carbon into the pathway by the addition of a DOXP synthase (Figure 1) and pulling more carbon out of the pathway into the required isoprenoid pyrophosphate building block, both of which are rate limiting steps in the MEP pathway (Table 1).[126] When this type of MEP pathway engineering was done for heterologous limonene production in *Synechocystis*, production was only seen to increase 1.36-fold.[127] In the unrelated *Anabena* sp. PCC 7120, production increased 2.3-fold in comparable environmental conditions, although at substantially lower titres.[68]

When this strategy was followed in *E. coli* for amorphadiene (a sesquiterpene) production, the production increase was comparable, at a 3.6-fold improvement.[6] When heterologous expression of a MVA pathway was carried out rather than targeted improvement to the endogenously regulated MEP pathway, amorphadiene yield increased a further 10-fold.[6]

A large proportion of published work in this area with cyanobacteria has focused on generating a basic strain that produces a specified isoprenoid and improving production by means other than metabolic engineering. Demonstrating increased production titres under higher light conditions or specialised photobioreactor designs are common strategies for this.[66–

[68,78,128,129] Given the relatively low titre improvements demonstrated under standard laboratory conditions in cyanobacteria, significant gains can be expected in the future. A variety of early efforts in improving MVA-based isoprenoid production in *E. coli* readily generated improvements, including order-of-magnitude production increases.[6,100,101,103] As has been demonstrated, only over-expressing of enzymes is not always the best choice in pathway engineering if the efficiency of that reaction is not optimised for the context it is occurring in.[100] At the most basic level, the production host and even growth stage of the host can impact functioning of an enzyme. Some effective improvement strategies have included balancing off-target effects by cell-wide functional genomics analysis, screening enzyme variants for optimal context-dependent kinetics and cofactor use, and reduction of metabolic burden by physically associating pathways to synthetic protein scaffolds for improved efficiency.[101–103]

Examination of metabolic intermediates in isoprenoid biosynthesis

I am currently unaware of any studies examining heterologous mevalonate production in cyanobacteria, particularly those closely related to *S. elongatus*. Determining the concentrations of intermediate metabolites can provide insight into flux bottlenecks in a pathway.

In the upper MVA *HMGR* variants tested using *E. coli* by Ma et al., including the *S. aureus* variant used in this study, the measured mevalonate concentration roughly correlated to concentration of the final heterologous isoprenoid molecule.[103] My measurements in *S. elongatus* showed a maximum mevalonate concentration of 70μM. While not atypical of results shown in photosynthetic systems, the reported mevalonate concentration using the same system in *E. coli* was more than 30-fold higher.[103]

When isoprene production was carried out in *Synechocystis* by Bentley *et al.*, the addition of a different complete MVA pathway only increased isoprene production from 1.9 to 4.7μM.[67] As one isoprene unit is generated per molecule of mevalonate, this suggests the MVA pathway used by the authors operates at a lower efficiency than the MVA pathway tested here. (Isoprene is rapidly lost into the headspace and is unlikely to be implicated in reduced pathway efficiency.) The authors chose to construct a MVA pathway with parts of bacterial origin to increase the chances of functional expression in their host and, the chosen isoprene synthase plus MVA pathway had been previously used in *E. coli*. In *E. coli*, introduction of the MVA pathway

resulted in an order of magnitude improvement.[130] In *Synechocystis*, the authors reassembled the pathway with different transcription/translation control sequences. The reassembly of their pathway may have resulted in a negative effect on its efficiency in the new host and correspondingly poor increase in isoprene production. Additionally, although the MVA genes were shown to be functional in *E. coli*, and protein accumulation was shown in *Synechocystis*, it is possible the new host exerted an unobserved regulatory effect on one of the translated proteins.

When a complete MVA pathway was expressed in the *S. elongatus* host, total measured β-carotene content (the major isoprenoid sink) was maximally 3μM (24μM mevalonate equivalent) higher than the wild type (Figure 11). If β-carotene was the only available carbon sink, it would suggest a pathway bottleneck. Since limited regulatory feedback from the cell on the heterologous MVA pathway can be expected, it is likely any negative regulation is occurring in the endogenous carotenoid pathway or that the carbon is being distributed more broadly to other endogenous isoprenoid derivatives. These would include pigments normally found in lower relative abundance and to phytol for chlorophyll a biosynthesis.

Because additional fixed carbon, ATP, and reducing equivalents are consumed by the MVA pathway (Figure 1), more must be generated to ensure regular functioning of the cell. Under light saturating conditions, significant growth defects when pulling fixed carbon into an engineered sink molecule are uncommon. When a carbon sink is present, increased photosystem II activity has been recorded (as measured by oxygen evolution).[68] While I did not measure rate changes in oxygen evolution, it would not be unreasonable to assume that the expressing the MVA pathway alone could also result in increased oxygen evolution. Expression of only the MVA pathway still diverts fixed carbon and energy away from endogenously regulated processes. This would necessitate increased photosynthetic activity to maintain a consistent growth rate.

The maximal production of 70μM of mevalonate in *S. elongatus* was done with the P_{LAC} promoter. While functional, P_{LAC} is known to be a weak foreign promoter in cyanobacterial systems. The demonstrated plasticity in cyanobacterial systems to fulfill the carbon and energy needs saturating light conditions suggests that use of a stronger foreign promoter would cause a corresponding increase in flux through the MVA pathway.

When the full MVA pathway was expressed here in *S. elongatus*, a small growth rate defect was detectable. As carbon, ATP, and NADPH do not seem to be limiting factors, the two most likely possibilities appear to be limited availability of transcription/translation machinery, or more likely, increased burden from continued selective pressure with two antibiotics.

Addition of the inducer IPTG had no apparent effect on mevalonate product levels. This suggests that although P_{LAC} can drive transcription in *S. elongatus*, the lac repressor is ineffective in this context with P_{LAC}.

Curiously, in two out of the four strain lineages a deficiency in mevalonate production was clearly present. In the analysis I reclassified the cultures from uninduced/induced to low/high expressing. If we assume a proportional increase in mevalonate concentrations with pathway copy number, the data suggests complete chromosome segregation occurred in only two of the lineages. Mean maximum mevalonate concentrations are approximately 4-fold greater in the high expressing cultures. Given that the median (and modal) number of chromosomes is 4 copies per cell (with approximately $^1/_3$ of cells having 4 copies) it is likely the low expressing lineages were only carrying one correct chromosome per cell on average.[97] Gene dosage has previously been described as a design concern for systems in another cyanobacterial polyploid, *Synechocystis* sp. PCC 6803.[109]

Relationship between chlorophyll, carotenoids, and isoprenoid flux

When I assessed chlorophyll a production in *S. elongatus* after the addition of a MVA pathway I saw the engineered cells maintained an equivalent per cell quantity of chlorophyll compared to the wild type during log phase (18 hours; Figure 10). The lower total chlorophyll quantity in the MVA strain at this time point can be attributed to the slightly lower rate of growth of the strain.

As the strains exit their log phase growth, per cell chlorophyll content drops by more than 25% in the wild type strain while the MVA containing strain maintains its per cell chlorophyll content (Figure 10). For the remainder of the measured time points chlorophyll content gradually decreases in both strains, but the per cell values for the MVA containing strain remain at least 20% higher than the wild type. It could be presumed that the retention of higher per cell

chlorophyll concentrations is due to the increased requirements for fixed carbon, ATP, and reducing equivalents by an active MVA pathway. The decreased chlorophyll concentration in the wild type can likely be considered a quantity sufficient for housekeeping once biomass generation begins to slow down.

The β-carotene concentrations display a similar trend of staying higher in the MVA strain after entering late log phase (Figure 11). However, unlike the equal amounts seen with chlorophyll, more β-carotene is seen on a per cell basis at the first time point in the MVA stain. This suggests that the regulation of carotenoid biosynthesis is not as strict as with chlorophyll a. Consideration should also be given to the possibility that reduction of per cell β-carotene concentrations over time is due to self-shading within the culture and a reduced need for photo-protection.

No clear trend is apparent in the ratio of β-carotene to chlorophyll over time in either strain. This ratio stays relatively consistent for the wild type strain at all time points. This suggests that β-carotene content is directly linked to the requirements of the photosystems for it in the wild type strain under the light intensity used here. The greater β-carotene content relative to chlorophyll in the MVA strain reinforces the idea that β-carotene can be assumed to be a sink for the additional flux of isoprenoids precursors generated by the MVA pathway and changes to chlorophyll levels are related to the level of photosystem activity required to meet the metabolic demands of the cell.

***S. elongatus* permeability to metabolites**

In the lower MVA pathway strain, I was unable to generate a co-transformant containing a heterologous farnesene synthase that could act as a carbon sink. Because of this, to assay the functionality of the lower pathway alone, I chose to screen for consumption of mevalonate rather than product formation.

When fed with mevalonate, no reduction in mevalonate concentration was detectable in the cultures (Figure 8). This effect has two likely causes. The first potential cause is pathway inactivity, either by extremely low processivity by the yeast mevalonate kinase (*ERG12*) in *S. elongatus* or knockdown by the heterologous host.

While *ERG12* catalyzes an ATP consuming reaction it is unlikely that ATP availability would limit this reaction. No significant growth defect was seen during strain growth. Additionally, increased metabolic burden on cyanobacteria appears to be linked with increased photosystem I activity - directly resulting in higher ATP production rates.[20,67,68] Additionally, the enzyme's reaction kinetics (in yeast) are not favourable for reversal of production formation.[131] While knockdown of the genes by the host is a possibility, this is not reported as a common occurrence in *S. elongatus*, unlike model eukaryotic algae such as *Chlamydomonas reinhardtii* which carry out RNA interference.[132]

The second, and more likely, potential cause of no apparent reduction in mevalonate concentration is limited substrate availability within the cells. This low availability in the fed substrate assay may be due to very low efficiency of metabolite membrane permeability in *S. elongatus*. The annotated genome of *S. elongatus* lists the majority of transporters as being involved with metal ions, as well as the type II secretion system for peptides.[123] Low membrane permeability has been previously demonstrated for small metabolites (lactate, fructose, glucose) in *S. elongatus*.[48] (Contrary to the higher membrane permeability seen for the same weak acid {lactate} in Synechocystis.[50]) When the relevant transporter was transformed into *S. elongatus*, membrane permeability issues were eliminated for the metabolite. In the case of an added hexose sugar transporter, *S. elongatus* cells were even able to sustain heterotrophic growth in dark conditions.

The addition of a transporter for mevalonate along with the lower MVA pathway would help to provide better insight into membrane permeability of heterologous metabolites in *S. elongatus*. Without the inclusion of a functional transporter, the use of radio-labelled mevalonate fed at much higher concentrations may be the most effective experimental option to probe this issue.

Biofilm formation

I attempted to reproduce a biofilm phenotype demonstrated in *S. elongatus* by Schatz *et al*, but was unsuccessful with my knockout strategy. I was most likely unable to fully segregate any transformants to a homo-polyploid state. Any remaining genome copies without the knockout would remain capable of secreting the presumed biofilm self-inhibitory small molecule/peptide.

Additionally, the authors had demonstrated the expression of two endogenous genes (Synpcc7942_1133 and Synpcc7942_1134) were necessary in addition to the knockout to generate the desired phenotype. While I did not validate protein expression for these genes in my strain, expression would be expected in the wild type stock unless a random inactivating mutation occurred in the original stock.

I am currently unaware of any laboratories that have reproduced the results generated, but the experiments used to characterise the cause of the phenotype appear well controlled. As the publication did not specify the origin or age of their *S. elongatus* stock, the clearest additional validation experiment for the phenotype's cause may be a whole genome analysis against the current reference genome.

Design-build-test cycles in S. elongatus

In my attempt to add this model organism to the collection of those already in use in our laboratory, I experienced multiple challenges with technical procedures specific to *S. elongatus*.

I initially experienced non-viable transformation efficiencies when using the common natural transformation method for *S. elongatus*. I was unable to determine the cause of the low efficiency and switched to using the more robust tri-parental mating method. While marginally more labour intensive, the gain in transformation efficiency was a necessity. While electroporation can be carried out in some cyanobacteria species (*Synechocystis* PCC6803, *Nostoc* PCC 7120,) it has not been demonstrated in *Synechococcus elongatus* PCC 7942.[46]

Even with a robust transformation method, contamination of strains by environmental microbes was a recurring concern. Cultures could have no apparent contaminating growth at inoculation, but become unusable over their period of growth as additional carbon was fixed photosynthetically. The slow growth rate of *S. elongatus* made this problematic as the cyanobacteria were not able to multiply at a rate that would make contaminating heterotrophs a negligible issue. As done here, and in other laboratories, the most effective method to manage this challenge appears to be frequently spotting the cultures onto heterotrophic media to screen for heterotrophic contaminants.[48]

The need to maintain strains in liquid culture for ease of use likely aggravates this issue. When putative transformants are picked from solid media they are first transferred to a small volume starter culture (typically a 24-well plate) before passaging the viable cultures into larger volumes. The recovery of strains from frozen stocks requires a similarly lengthy process.

The slow rate of growth also made attempting to separate out the desired strain from contaminating colonies on solid media highly challenging. In my experience, once the culture was identified as contaminated, heterotrophic colonies would form at a high enough rate on photoautotrophic solid media that the *S. elongatus* colonies could not be easily picked without carrying contaminating cells over. Attempting to mechanically separate the cell types by streaking proved similarly problematic.

CRISPR-Cas facilitated engineering presents an interesting opportunity to speed up the engineering cycle in *Synechococcus elongatus* PCC 7942 and other polyploids with random genome segregation.[133,134] *S. elongatus* has no known CRISPR-Cas system that could be repurposed for genome editing, making the addition of a heterologous construct necessary.[135]

A 'clonal' population following a transformation protocol is *Synechococcus elongatus* PCC 7942 can result in cells within the population having between 0-100% of their genomes containing the integration of interest. This mixed population can maintain itself in culture, or result in the complete gain or loss of the genome of interest following further culturing. To achieve a true clonal population, repeated sub-culturing can be required.

Traditional integration tools for *Synechococcus elongatus* PCC 7942 rely on large homology regions for their efficiency.[96] These regions are typically seen in practice ranging from 500-1500bp. Targeted CRISPR-Cas cutting of the genome in regions expected to be ablated by an integration event could eliminate additional weeks sub-culturing and potentially reduce the required size of the homology regions for efficient transformations. Additionally, knockouts would be able to propagate immediately within a cell's multiple genomes from only a single copy of the required CRISPR-Cas guide RNAs.

As also discussed by others, the two areas required for increased reliability in cyanobacterial engineering are better understood parts and more efficient tools. Much like with more unrelated species groups, inferences can not necessarily be made about part functionality in one

cyanobacterial species from data collected in another. Multiple review articles have attempted to compile part data sheets out of the existing literature, but little quantitative or context-normalised data is available still. While successful approaches to faster genome modification in *S. elongatus* will undoubtedly appear, the biggest hurdle to rapid engineering of model photoautotrophic cyanobacterial systems remains growth rate.

I am hopeful that further characterisation of the fast growing *Synechococcus elongatus* UTEX 2973 species will result in its greater use as a host species for engineered systems, and that the better comprehension of its biology can be used to enhance our understanding of carbon partitioning regulation in other related species and possibly even improve their growth rates.

References

1. Chang, J. *Green Chemicals: Biomass chemicals to be competitive in 10–15 years*. (2012). at <http://www.icis.com/Articles/2012/04/02/9546230/green-chemicals-biomass-chemicals-to-be-competitive-in-1015.html>
2. *Proceedings of the Twenty-Fifth Symposium on Biotechnology for Fuels and Chemicals Held May 4–7, 2003, in Breckenridge, CO*. (Humana Press, 2004). doi:10.1007/978-1-59259-837-3
3. Gallezot, P. Conversion of biomass to selected chemical products. *Chem. Soc. Rev.* **41,** 1538–58 (2012).
4. Yadav, V. G., De Mey, M., Giaw Lim, C., Kumaran Ajikumar, P. & Stephanopoulos, G. The future of metabolic engineering and synthetic biology: Towards a systematic practice. *Metab. Eng.* **14,** 233–241 (2012).
5. Koffas, M., Roberge, C., Lee, K. & Stephanopoulos, G. Metabolic engineering. *Annu. Rev. Biomed. Eng.* **1,** 535–57 (1999).
6. Martin, V. J. J., Pitera, D. J., Withers, S. T., Newman, J. D. & Keasling, J. D. Engineering a mevalonate pathway in Escherichia coli for production of terpenoids. *Nat. Biotechnol.* **21,** 796–802 (2003).
7. Ro, D.-K. *et al.* Production of the antimalarial drug precursor artemisinic acid in engineered yeast. *Nature* **440,** 940–3 (2006).
8. Yim, H. *et al.* Metabolic engineering of Escherichia coli for direct production of 1,4-butanediol. *Nat. Chem. Biol.* **7,** 445–52 (2011).
9. Wang, C. *et al.* Farnesol production from Escherichia coli by harnessing the exogenous mevalonate pathway. *Biotechnol. Bioeng.* **107,** 421–9 (2010).
10. Wu, S. & Chappell, J. Metabolic engineering of natural products in plants; tools of the trade and challenges for the future. *Curr. Opin. Biotechnol.* **19,** 145–52 (2008).
11. Serra, T. & Zilberman, D. Biofuel-related price transmission literature: A review. *Energy Econ.* **37,** 141–151 (2013).
12. Hays, S. G. & Ducat, D. C. Engineering cyanobacteria as photosynthetic feedstock factories. *Photosynth. Res.* **123,** 285–95 (2015).
13. Bridgwater, A. V. Review of fast pyrolysis of biomass and product upgrading. *Biomass and Bioenergy* **38,** 68–94 (2012).
14. Chiaramonti, D., Prussi, M., Buffi, M., Rizzo, A. M. & Pari, L. Review and experimental study on pyrolysis and hydrothermal liquefaction of microalgae for biofuel production. *Appl. Energy* (2016). doi:10.1016/j.apenergy.2015.12.001
15. Daroch, M., Geng, S. & Wang, G. Recent advances in liquid biofuel production from algal feedstocks. *Appl. Energy* **102,** 1371–1381 (2013).
16. Martone, P. T. *et al.* Discovery of lignin in seaweed reveals convergent evolution of cell-wall architecture. *Curr. Biol.* **19,** 169–75 (2009).

17. Elliott, D. C. *et al.* Process development for hydrothermal liquefaction of algae feedstocks in a continuous-flow reactor. *Algal Res.* **2,** 445–454 (2013).

18. Miao, X. & Wu, Q. Biodiesel production from heterotrophic microalgal oil. *Bioresour. Technol.* **97,** 841–6 (2006).

19. Rodolfi, L. *et al.* Microalgae for oil: strain selection, induction of lipid synthesis and outdoor mass cultivation in a low-cost photobioreactor. *Biotechnol. Bioeng.* **102,** 100–12 (2009).

20. Ducat, D. C., Avelar-Rivas, J. A., Way, J. C. & Silver, P. A. Rerouting carbon flux to enhance photosynthetic productivity. *Appl. Environ. Microbiol.* **78,** 2660–8 (2012).

21. Deng, M. D. & Coleman, J. R. Ethanol synthesis by genetic engineering in cyanobacteria. *Appl. Environ. Microbiol.* **65,** 523–8 (1999).

22. Liu, X., Sheng, J. & Curtiss, R. Fatty acid production in genetically modified cyanobacteria. *Proc. Natl. Acad. Sci. U. S. A.* **108,** 6899–904 (2011).

23. Kovacevic, V. & Wesseler, J. Cost-effectiveness analysis of algae energy production in the EU. *Energy Policy* **38,** 5749–5757 (2010).

24. Melis, A. Solar energy conversion efficiencies in photosynthesis: Minimizing the chlorophyll antennae to maximize efficiency. *Plant Sci.* **177,** 272–280 (2009).

25. Reshes, G., Vanounou, S., Fishov, I. & Feingold, M. Timing the start of division in E. coli: a single-cell study. *Phys. Biol.* **5,** 046001 (2008).

26. Di Talia, S., Skotheim, J. M., Bean, J. M., Siggia, E. D. & Cross, F. R. The effects of molecular noise and size control on variability in the budding yeast cell cycle. *Nature* **448,** 947–51 (2007).

27. Savage, D. F., Afonso, B., Chen, A. H. & Silver, P. A. Spatially ordered dynamics of the bacterial carbon fixation machinery. *Science* **327,** 1258–61 (2010).

28. Yu, J. *et al.* Synechococcus elongatus UTEX 2973, a fast growing cyanobacterial chassis for biosynthesis using light and CO2. *Sci. Rep.* **5,** 8132 (2015).

29. Goulding, K. H. & Merrett, M. J. The Photometabolism of Acetate by Chlorella pyrenoidosa. *J. Exp. Bot.* **17,** 678–689 (1966).

30. Greene, R. M., Geider, R. J., Kolber, Z. & Falkowski, P. G. Iron-induced changes in light harvesting and photochemical energy conversion processes in eukaryotic marine algae. *Plant Physiol.* **100,** 565–75 (1992).

31. Lynch, D. V & Thompson, G. A. Low Temperature-Induced Alterations in the Chloroplast and Microsomal Membranes of Dunaliella salina. *Plant Physiol.* **69,** 1369–75 (1982).

32. A ! Realistic ! Technology ! and ! Engineering ! Assessment ! of ! Algae ! Biofuel ! Production ! (2010).

33. *Handbook of Microalgal Culture: Biotechnology and Applied Phycology*. (2007). doi:10.1002/9780470995280

34. Jiménez, C., Cossío, B. R., Labella, D. & Niell, F. X. The Feasibility of industrial production of Spirulina (Arthrospira) in Southern Spain. *Aquaculture* **217,** 179–190 (2003).

35. Gendy, T. S. & El-Temtamy, S. A. Commercialization potential aspects of microalgae for biofuel production: An overview. *Egypt. J. Pet.* **22,** 43–51 (2013).

36. Ooms, M. D. *et al.* Evanescent photosynthesis: exciting cyanobacteria in a surface-confined light field. *Phys. Chem. Chem. Phys.* **14,** 4817–23 (2012).

37. Iwamura, T. Change of nucleic acid content in Chlorella cells during the course of their life-cycle. *J. Biochem.* **42,** 575–589 (1955).

38. Curtain, C., Looney, F., Regan, D. & Ivancic, M. Changes in the ordering of lipids in the membrane of Dunaliella in response to osmotic-pressure changes. An e.s.r. study. *Biochem. J.* (1983). at <http://www.biochemj.org/bj/213/bj2130131.htm>

39. Jensen, P. E. & Leister, D. Cyanobacteria as an Experimental Platform for Modifying Bacterial and Plant Photosynthesis. *Front. Bioeng. Biotechnol.* **2,** 7 (2014).

40. Ducat, D. C., Sachdeva, G. & Silver, P. A. Rewiring hydrogenase-dependent redox circuits in cyanobacteria. *Proc. Natl. Acad. Sci. U. S. A.* **108,** 3941–6 (2011).

41. Aasen, A. J., Eimhjellen, K. E. & Liaaen-Jensen, S. An extreme source of beta-carotene. *Acta Chem. Scand.* **23,** 2544–5 (1969).

42. Ben-Amotz, A., Katz, A. & Avron, M. Accumulation of β-carotene in halotolerant algae: Purification and characterization of β-carotene-rich globules from Dunaliella bardawil (Chlorophyceae). *J. Phycol.* **18,** 529–537 (1982).

43. Lagarde, D., Beuf, L. & Vermaas, W. Increased Production of Zeaxanthin and Other Pigments by Application of Genetic Engineering Techniques to Synechocystis sp. Strain PCC 6803. *Appl. Environ. Microbiol.* **66,** 64–72 (2000).

44. *The Cyanobacteria : Molecular Biology, Genomics, and Evolution*. (Caister Academic Press, 2008). at <https://encore.concordia.ca/iii/encore/record/C__Rb2536631?lang=eng&suite=def>

45. Kondo, T. *et al.* Circadian clock mutants of cyanobacteria. *Science* **266,** 1233–6 (1994).

46. Heidorn, T. *et al. Synthetic biology in cyanobacteria engineering and analyzing novel functions. Methods Enzymol.* **497,** (2011).

47. Aikens, J. & Turner, R. J. Transgenic photosynthetic microorganisms and photobioreactor. (2013). at <http://patft.uspto.gov/netacgi/nph-Parser?Sect2=PTO1&Sect2=HITOFF&p=1&u=/netahtml/PTO/search-bool.html&r=1&f=G&l=50&d=PALL&RefSrch=yes&Query=PN/8367379>

48. Niederholtmeyer, H., Wolfstädter, B. T., Savage, D. F., Silver, P. A. & Way, J. C. Engineering cyanobacteria to synthesize and export hydrophilic products. *Appl. Environ. Microbiol.* **76,** 3462–6 (2010).

49. Angermayr, S. A. *et al.* Exploring metabolic engineering design principles for the photosynthetic production of lactic acid by Synechocystis sp. PCC6803. *Biotechnol.*

Biofuels **7,** 99 (2014).

50. Angermayr, S. A., Paszota, M. & Hellingwerf, K. J. Engineering a cyanobacterial cell factory for production of lactic acid. *Appl. Environ. Microbiol.* **78,** 7098–106 (2012).

51. Lamers, P. P. *et al.* Carotenoid and fatty acid metabolism in light-stressed Dunaliella salina. *Biotechnol. Bioeng.* **106,** 638–48 (2010).

52. Blumwald, E., Mehlhorn, R. J. & Packer, L. Studies of osmoregulation in salt adaptation of cyanobacteria with ESR spin-probe techniques. *Proc. Natl. Acad. Sci. U. S. A.* **80,** 2599–602 (1983).

53. Miao, X., Wu, Q., Wu, G. & Zhao, N. Sucrose accumulation in salt-stressed cells of agp gene deletion-mutant in cyanobacterium Synechocystis sp PCC 6803. *FEMS Microbiol. Lett.* **218,** 71–7 (2003).

54. Martínez-Noël, G. M. A. *et al.* First evidence of sucrose biosynthesis by single cyanobacterial bimodular proteins. *FEBS Lett.* **587,** 1669–74 (2013).

55. Agapakis, C. M. *et al.* Towards a synthetic chloroplast. *PLoS One* **6,** e18877 (2011).

56. Rude, M. a & Schirmer, A. New microbial fuels: a biotech perspective. *Curr. Opin. Microbiol.* **12,** 274–81 (2009).

57. Guerrero, F., Carbonell, V., Cossu, M., Correddu, D. & Jones, P. R. Ethylene synthesis and regulated expression of recombinant protein in Synechocystis sp. PCC 6803. *PLoS One* **7,** e50470 (2012).

58. Ogawa, T., Takahashi, M., Fujii, T., Tazaki, M. & Fukuda, H. The Role of NADH:Fe(III)EDTA Oxidoreductase in Ethylene Formation from 2-Keto-4-Methylthiobutyrate. *J. Ferment. Bioeng.* **69,** 287–291 (1990).

59. Ungerer, J. *et al.* Sustained photosynthetic conversion of CO2 to ethylene in recombinant cyanobacterium Synechocystis 6803. *Energy Environ. Sci.* **5,** 8998 (2012).

60. Atsumi, S., Higashide, W. & Liao, J. C. Direct photosynthetic recycling of carbon dioxide to isobutyraldehyde. *Nat. Biotechnol.* **27,** 1177–80 (2009).

61. Shen, C. R. & Liao, J. C. Photosynthetic production of 2-methyl-1-butanol from CO2 in cyanobacterium Synechococcus elongatus PCC7942 and characterization of the native acetohydroxyacid synthase. *Energy Environ. Sci.* **5,** 9574 (2012).

62. Morrison, S. S., Mullineaux, C. W. & Ashby, M. K. The influence of acetyl phosphate on DspA signalling in the Cyanobacterium Synechocystis sp. PCC6803. *BMC Microbiol.* **5,** 47 (2005).

63. Wang, W., Liu, X. & Lu, X. Engineering cyanobacteria to improve photosynthetic production of alka(e)nes. *Biotechnol. Biofuels* **6,** 69 (2013).

64. Hu, P. *et al.* Metabolic phenotyping of the cyanobacterium Synechocystis 6803 engineered for production of alkanes and free fatty acids. *Appl. Energy* **102,** 850–859 (2013).

65. Lindberg, P., Park, S. & Melis, A. Engineering a platform for photosynthetic isoprene production in cyanobacteria, using Synechocystis as the model organism. *Metab. Eng.* **12,**

70–9 (2010).

66. Bentley, F. K. & Melis, A. Diffusion-based process for carbon dioxide uptake and isoprene emission in gaseous/aqueous two-phase photobioreactors by photosynthetic microorganisms. *Biotechnol. Bioeng.* **109,** 100–9 (2012).

67. Bentley, F. K., Zurbriggen, A. & Melis, A. Heterologous expression of the mevalonic acid pathway in cyanobacteria enhances endogenous carbon partitioning to isoprene. *Mol. Plant* **7,** 71–86 (2014).

68. Halfmann, C., Gu, L. & Zhou, R. Engineering cyanobacteria for the production of a cyclic hydrocarbon fuel from CO2 and H2O. *Green Chem.* **16,** 3175 (2014).

69. Jacobsen, J. H. & Frigaard, N.-U. Engineering of photosynthetic mannitol biosynthesis from CO2 in a cyanobacterium. *Metab. Eng.* **21,** 60–70 (2014).

70. Berg, A., Lindblad, P. & Svensson, B. H. Cyanobacteria as a source of hydrogen for methane formation. *World J. Microbiol. Biotechnol.* **30,** 539–45 (2014).

71. Takahama, K., Matsuoka, M., Nagahama, K. & Ogawa, T. Construction and analysis of a recombinant cyanobacterium expressing a chromosomally inserted gene for an ethylene-forming enzyme at the psbAI locus. *J. Biosci. Bioeng.* **95,** 302–305 (2003).

72. Sakai, M., Ogawa, T., Matsuoka, M. & Fukuda, H. Photosynthetic conversion of carbon dioxide to ethylene by the recombinant cyanobacterium, Synechococcus sp. PCC 7942, which harbors a gene for the ethylene-forming enzyme of Pseudomonas syringae. *J. Ferment. Bioeng.* **84,** 434–443 (1997).

73. Zhu, T., Xie, X., Li, Z., Tan, X. & Lu, X. Enhancing photosynthetic production of ethylene in genetically engineered Synechocystis sp. PCC 6803. *Green Chem.* (2014). doi:10.1039/C4GC01730G

74. Dexter, J. & Fu, P. Metabolic engineering of cyanobacteria for ethanol production. *Energy Environ. Sci.* **2,** 857 (2009).

75. Ruffing, A. M. & Jones, H. D. T. Physiological effects of free fatty acid production in genetically engineered Synechococcus elongatus PCC 7942. *Biotechnol. Bioeng.* **109,** 2190–9 (2012).

76. Ruffing, A. M. Improved Free Fatty Acid Production in Cyanobacteria with Synechococcus sp. PCC 7002 as Host. *Front. Bioeng. Biotechnol.* **2,** (2014).

77. Reppas, N. B. ; & Ridley, C. P. Methods and compositions for the recombinant biosynthesis of n-alkanes. (2013). at <https://www.google.ca/patents/US8481285?dq=Methods+and+compositions+for+the+recombinant+biosynthesis+of+n-alkanes&hl=en&sa=X&ei=RZFMVK3tNc2wyATM9YLACw&ved=0CDEQ6AEwAw>

78. Halfmann, C., Gu, L., Gibbons, W. & Zhou, R. Genetically engineering cyanobacteria to convert CO2, water, and light into the long-chain hydrocarbon farnesene. *Appl. Microbiol. Biotechnol.* (2014). doi:10.1007/s00253-014-6118-4

79. Lange, B. M., Rujan, T., Martin, W. & Croteau, R. Isoprenoid biosynthesis: the evolution of two ancient and distinct pathways across genomes. *Proc. Natl. Acad. Sci. U. S. A.* **97,**

13172–7 (2000).

80. Sacchettini, J. C. & Poulter, C. D. Creating Isoprenoid Diversity. *Science (80-.).* **277,** 1788–1789 (1997).

81. Which Fuels for Low CO2 Engines?: Proceedings of the International Conference Held in Rueil-Malmaison, France, September, 22-23, 2004. in *IFP Int. Conf.* (Duret, P. & Montagne, X.) 233 (Editions TECHNIP, 2004). at <http://books.google.com/books?hl=en&lr=&id=OPecQt9Fc-kC&pgis=1>

82. Harvey, B. G., Wright, M. E. & Quintana, R. L. High-Density Renewable Fuels Based on the Selective Dimerization of Pinenes. *ACS Energy Fuels* (2010). doi:10.1021/ef900799c

83. Sarria, S., Wong, B., García Martín, H., Keasling, J. D. & Peralta-Yahya, P. Microbial synthesis of pinene. *ACS Synth. Biol.* **3,** 466–75 (2014).

84. Fisher, K., Schofer, S. J. & Kanne, D. B. Squalane and isosqualane compositions and methods for preparing the same. (2013). at <https://www.google.ca/patents/US8586814?dq=industrial+%22farnesene%22+use+amyris&hl=en&sa=X&ved=0ahUKEwiI2s79pYrLAhVBdT4KHTI0CekQ6AEIMDAD>

85. McPhee, D. J. & Graham, M. J. Adhesive compositions comprising a polyfarnesene. (2010). at <https://www.google.ca/patents/US7655739?dq=industrial+%22farnesene%22+use+amyris&hl=en&sa=X&ved=0ahUKEwiFxqWTporLAhXMaD4KHVtsDOk4FBDoAQgoMAI>

86. McPhee, D. J. Farnesene interpolymers. (2012). at <https://www.google.ca/patents/US8217128?dq=industrial+%22farnesene%22+use+amyris&hl=en&sa=X&ved=0ahUKEwiI2s79pYrLAhVBdT4KHTI0CekQ6AEINzAE>

87. Alper, H. & Stephanopoulos, G. Engineering for biofuels: exploiting innate microbial capacity or importing biosynthetic potential? *Nat. Rev. Microbiol.* **7,** 715–23 (2009).

88. Dietrich, J. A., McKee, A. E. & Keasling, J. D. High-throughput metabolic engineering: advances in small-molecule screening and selection. *Annu. Rev. Biochem.* **79,** 563–90 (2010).

89. Harker, M. & Bramley, P. M. Expression of prokaryotic 1-deoxy-d-xylulose-5-phosphatases in Escherichia coli increases carotenoid and ubiquinone biosynthesis. *FEBS Lett.* **448,** 115–119 (1999).

90. Kim, S. W. & Keasling, J. D. Metabolic engineering of the nonmevalonate isopentenyl diphosphate synthesis pathway in Escherichia coli enhances lycopene production. *Biotechnol. Bioeng.* **72,** 408–15 (2001).

91. Alper, H., Miyaoku, K. & Stephanopoulos, G. Construction of lycopene-overproducing E. coli strains by combining systematic and combinatorial gene knockout targets. *Nat. Biotechnol.* **23,** 612–6 (2005).

92. Yoon, S.-H. *et al.* Increased beta-carotene production in recombinant Escherichia coli harboring an engineered isoprenoid precursor pathway with mevalonate addition. *Biotechnol. Prog.* **23,** 599–605

93. Özaydın, B., Burd, H., Lee, T. S. & Keasling, J. D. Carotenoid-based phenotypic screen of

the yeast deletion collection reveals new genes with roles in isoprenoid production. *Metab. Eng.* **15,** 174–83 (2013).

94. Vioque, A. Transformation of cyanobacteria. *Adv. Exp. Med. Biol.* **616,** 12–22 (2007).

95. Ruffing, A. M. Engineered cyanobacteria: Teaching an old bug new tricks. *Bioeng. Bugs* **2,** 136–149 (2011).

96. Clerico, E. M., Ditty, J. L. & Golden, S. S. Specialized techniques for site-directed mutagenesis in cyanobacteria. *Methods Mol. Biol.* **362,** 155–71 (2007).

97. Chen, A. H., Afonso, B., Silver, P. A. & Savage, D. F. Spatial and temporal organization of chromosome duplication and segregation in the cyanobacterium Synechococcus elongatus PCC 7942. *PLoS One* **7,** e47837 (2012).

98. Ooms, M. D., Erickson, D. & Sinton, D. Evanescent Cultivation of Cyanobacteria for Bioenergy. in *CLEO2011 - Laser Appl. to Photonic Appl.* (Optical Society of America, 2011). doi:10.1364/CLEO_SI.2011.CTuF6

99. Schatz, D. *et al.* Self-suppression of biofilm formation in the cyanobacterium Synechococcus elongatus. *Environ. Microbiol.* **15,** 1786–94 (2013).

100. Pitera, D. J., Paddon, C. J., Newman, J. D. & Keasling, J. D. Balancing a heterologous mevalonate pathway for improved isoprenoid production in Escherichia coli. *Metab. Eng.* **9,** 193–207 (2007).

101. Kizer, L., Pitera, D. J., Pfleger, B. F. & Keasling, J. D. Application of functional genomics to pathway optimization for increased isoprenoid production. *Appl. Environ. Microbiol.* **74,** 3229–41 (2008).

102. Dueber, J. E. *et al.* Synthetic protein scaffolds provide modular control over metabolic flux. *Nat. Biotechnol.* **27,** 753–9 (2009).

103. Ma, S. M. *et al.* Optimization of a heterologous mevalonate pathway through the use of variant HMG-CoA reductases. *Metab. Eng.* **13,** 588–97 (2011).

104. Wang, C. *et al.* Metabolic engineering of Escherichia coli for α-farnesene production. *Metab. Eng.* **13,** 648–55 (2011).

105. Marasco, E. Identification and characterization of bacterial carotenoid cleavage oxygenases. (2008). at <http://search.proquest.com/docview/304581863>

106. Schafer, L., Sandmann, M., Woitsch, S. & Sandmann, G. Coordinate up-regulation of carotenoid biosynthesis as a response to light stress in Synechococcus PCC7942. *Plant, Cell Environ.* **29,** 1349–1356 (2006).

107. Design and characterization of molecular tools for a Synthetic Biology approach towards developing cyanobacterial biotechnology. *Nucleic Acids Res.* **38,** 2577–93 (2010).

108. McEwen, J. T., Machado, I. M. P., Connor, M. R. & Atsumi, S. Engineering Synechococcus elongatus PCC 7942 for continuous growth under diurnal conditions. *Appl. Environ. Microbiol.* **79,** 1668–75 (2013).

109. Camsund, D. & Lindblad, P. Engineered transcriptional systems for cyanobacterial biotechnology. *Front. Bioeng. Biotechnol.* **2,** 40 (2014).

110. Geerts, D., Bovy, A., de Vrieze, G., Borrias, M. & Weisbeek, P. Inducible expression of heterologous genes targeted to a chromosomal platform in the cyanobacterium Synechococcus sp. PCC 7942. *Microbiology* **141 (Pt 4,** 831–41 (1995).

111. Lan, E. I. & Liao, J. C. Metabolic engineering of cyanobacteria for 1-butanol production from carbon dioxide. *Metab. Eng.* **13,** 353–63 (2011).

112. Mori, T. *et al.* Circadian clock protein KaiC forms ATP-dependent hexameric rings and binds DNA. *Proc. Natl. Acad. Sci. U. S. A.* **99,** 17203–8 (2002).

113. Sambrook, J. & Russell, D. W. *Molecular Cloning: A Laboratory Manual*. (CSHL Press, 2001). at <https://books.google.com/books?id=Bosc5JVxNpkC&pgis=1>

114. Seidman, C. E., Struhl, K., Sheen, J. & Jessen, T. Introduction of plasmid DNA into cells. *Curr. Protoc. Mol. Biol.* **Chapter 1,** Unit 1.8 (2001).

115. Horton, R. M., Cai, Z. L., Ho, S. N. & Pease, L. R. Gene splicing by overlap extension: Tailor-made genes using the polymerase chain reaction. *Biotechniques* **54,** 528–535 (2013).

116. Andersson, C. R. *et al. Application of bioluminescence to the study of circadian rhythms in cyanobacteria*. *Methods Enzymol.* **305,** (Elsevier, 2000).

117. Way, J. C., Niederholtmeyer, H., Wolfstaedter, B. & Savage, D. Production of secreted bioproducts from photosynthetic microbes. (2012). at <http://www.google.com/patents/US20120220007>

118. Amann, E., Ochs, B. & Abel, K. J. Tightly regulated tac promoter vectors useful for the expression of unfused and fused proteins in Escherichia coli. *Gene* **69,** 301–15 (1988).

119. Shestakov, S. V. & Khyen, N. T. Evidence for genetic transformation in blue-green alga Anacystis nidulans. *MGG Mol. Gen. Genet.* **107,** 372–375 (1970).

120. Niederhotmeyer, H. , personal communication.

121. Elhai, J., Vepritskiy, A., Muro-Pastor, A. M., Flores, E. & Wolk, C. P. Reduction of conjugal transfer efficiency by three restriction activities of Anabaena sp. strain PCC 7120. *J. Bacteriol.* **179,** 1998–2005 (1997).

122. Huang, H. Design and characterization of artificial transcriptional terminators. (2007). at <http://dspace.mit.edu/handle/1721.1/45981>

123. Copeland, A. *et al. Synechococcus elongatus PCC 7942, complete genome*. (2005). at <http://www.ncbi.nlm.nih.gov/nuccore/NC_007604>

124. Diego, S. & Jolla, L. Changes in the cyanobacterial photosynthetic apparatus during acclimation to macronutrient deprivation. 173–183 (1994).

125. Leavell, M. D., McPhee, D. J. & Paddon, C. J. Developing fermentative terpenoid production for commercial usage. *Curr. Opin. Biotechnol.* **37,** 114–9 (2016).

126. Angermayr, S. A., Gorchs Rovira, A. & Hellingwerf, K. J. Metabolic engineering of cyanobacteria for the synthesis of commodity products. *Trends Biotechnol.* **33,** 352–361 (2015).

127. Kiyota, H., Okuda, Y., Ito, M., Hirai, M. Y. & Ikeuchi, M. Engineering of cyanobacteria for the photosynthetic production of limonene from CO2. *J. Biotechnol.* **185,** 1–7 (2014).

128. Masamoto, K. & Furukawa, K. Accumulation of zeaxanthin in cells of the cyanobacterium, Synechococcus sp. Strain PCC 7942 grown under high irradiance. *J. Plant Physiol.* **151,** 257–261 (1997).

129. Kudoh, K. *et al.* Prerequisite for highly efficient isoprenoid production by cyanobacteria discovered through the over-expression of 1-deoxy-d-xylulose 5-phosphate synthase and carbon allocation analysis. *J. Biosci. Bioeng.* **118,** 20–8 (2014).

130. Zurbriggen, A., Kirst, H. & Melis, A. Isoprene Production Via the Mevalonic Acid Pathway in Escherichia coli (Bacteria). *BioEnergy Res.* **5,** 814–828 (2012).

131. Caspi, R. *et al.* The MetaCyc database of metabolic pathways and enzymes and the BioCyc collection of Pathway/Genome Databases. *Nucleic Acids Res.* **42,** D459–71 (2014).

132. Harris, E. H. *The Chlamydomonas Sourcebook: Introduction to Chlamydomonas and Its Laboratory Use, Volume 1*. (Academic Press, 2009). at <https://books.google.com/books?id=xTjJGV5GWY0C&pgis=1>

133. Charpentier, E. & Doudna, J. A. Biotechnology: Rewriting a genome. *Nature* **495,** 50–1 (2013).

134. Cong, L. *et al.* Multiplex genome engineering using CRISPR/Cas systems. *Science* **339,** 819–23 (2013).

135. Cai, F., Axen, S. D. & Kerfeld, C. A. *Evidence for the widespread distribution of CRISPR-Cas system in the Phylum Cyanobacteria*. *RNA Biol.* (Taylor & Francis, 2013). at <http://www.tandfonline.com/doi/full/10.4161/rna.24571>

136. Lee, R. E. *Phycology*. (Cambridge University Press, 2008). doi:10.1017/CBO9780511812897

Appendices

Non-commercial incubators

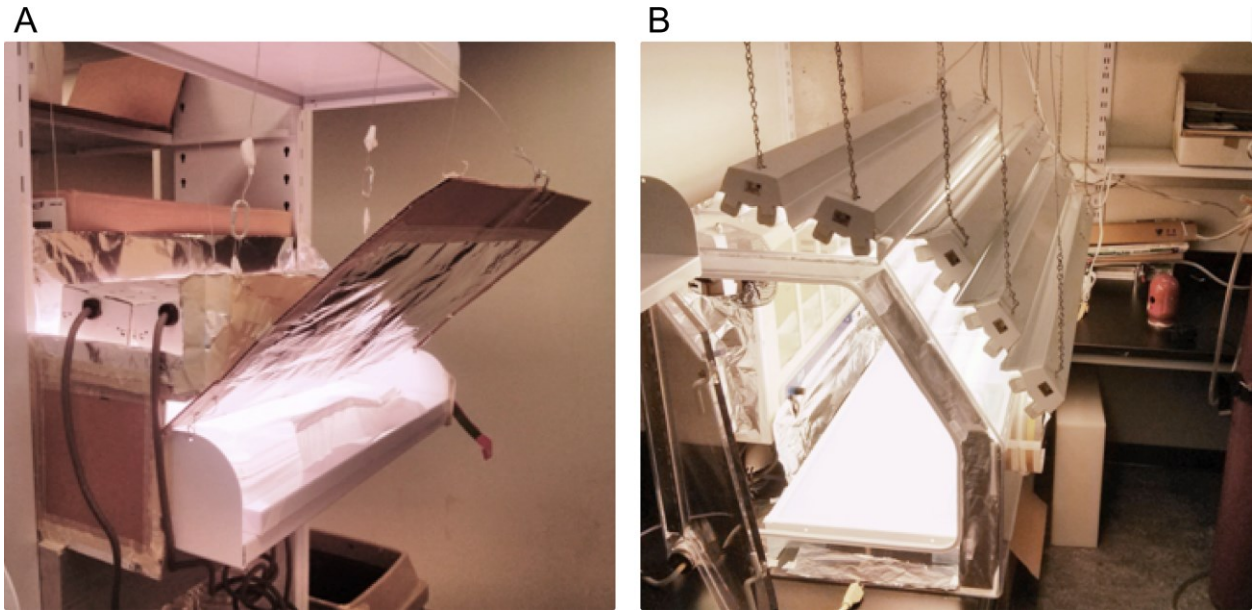

Supplementary Figure 1
Non-commercial incubators used for *S. elongatus* plates. (A) Small plate incubator. 34°C set point maintained from heat output of bulbs. Maximum 50µmol·$m^{-2}s^{-1}$ light output. (B) Converted anaerobic hood for plate incubation. Variable temperature set point. Variable atmospheric gas mixture possible. Maximum 70µmol·$m^{-2}s^{-1}$ light output.

Primer table

Supplementary Table 1. List of primers used

Primer	Sequence
ERG12_fwd	ATGTCATTACCGTTCTTAACTTCT
ERG12-nostop_rev	TGAAGTCCATGGTAAATTCGTG
ERG8_fwd	ATGTCAGAGTTGAGAGCCTT
ERG8-nostop_rev	TTTATCAAGATAAGTTTCCGGATCT
MVD1_fwd	ATGACCGTTTACACAGCATC
MVD1-nostop_rev	TTCCTTTGGTAGACCAGTCTTT
idi_fwd	ATGCAAACGGAACACGTC
idi-nostop_rev	TTTAAGCTGGGTAAATGCAGA
ispA_fwd	ATGGACTTTCCGCAGCAA
ispA-nostop_rev	TTTATTACGCTGGATGATGTAGT
atoB_fwd	ATGAAAAATTGTGTCATCGTCAGTGC
atoB-nostop_rev	ATTCAACCGTTCAATCACCATCG
ERG13_fwd	ATGAAACTCTCAACTAAACTTTGTTG
ERG13_rev	CTTATTTTTTAACATCGTAAGATCTTC
seqpsbA2aFS-f2	GCCAATCTGTTCGAAAAAGAAA
seqpsbA2aFS-r3	TGCCTGCACCACGTTAAAAT

Codon optimised HMGR-Sa sequence

```
LOCUS       pZW(NS1:MTSa)       8211 bp ds-DNA     circular
DEFINITION  .
FEATURES             Location/Qualifiers
     misc_recomb     744..1543
                     /label="NS1 CDS"
     CDS             1550..2694
                     /label="SpecR cassette CDS"
     misc_feature    2728..2757
                     /label="lacProm primer"
     misc_recomb     7431..8210
                     /label="NS1 CDS"
     CDS             2956..4137
                     /label="atoB CDS"
     CDS             5646..6926
                     /label="HMGR-Sa (codon optimised Staphylococcus aureus origin)"
     misc_feature    7332..7359
                     /label="rrnB T2 terminator primer"
     CDS             4154..5626
                     /label="ERG13 CDS"
ORIGIN
        1 gataatctca tgaccaaaat cccttaacgt gagttttcgt tccactgagc gtcagacccc
       61 gtagaaaaga tcaaaggatc ttcttgagat cctttttttc tgcgcgtaat ctgctgcttg
      121 caaacaaaaa aaccaccgct accagcggtg gtttgtttgc cggatcaaga gctaccaact
      181 ctttttccga aggtaactgg cttcagcaga gcgcagatac caaatactgt tcttctagtg
      241 tagccgtagt taggccacca cttcaagaac tctgtagcac cgcctacata cctcgctctg
      301 ctaatcctgt taccagtggc tgctgccagt ggcgataagt cgtgtcttac cgggttggac
      361 tcaagacgat agttaccgga taaggcgcag cggtcgggct gaacgggggg ttcgtgcaca
      421 cagcccagct tggagcgaac gacctacacc gaactgagat acctacagcg tgagctatga
      481 gaaagcgcca cgcttcccga agggagaaag gcggacaggt atccggtaag cggcagggtc
      541 ggaacaggag agcgcacgag ggagcttcca gggggaaacg cctggtatct ttatagtcct
      601 gtcgggtttc gccacctctg acttgagcgt cgatttttgt gatgctcgtc aggggggcgg
      661 agcctatgga aaaacgccag caacgcggcc tttttacggt tcctggcctt ttgctggcct
      721 tttgctcaca tgtgtgctgg gccccaatgc cttctccaag ggcggcattc cctgactgt
      781 tgaaggcgtt gccaatatca agattgctgg ggaagaaccg accatccaca acgcgatcga
      841 gcggctgctt ggcaaaaacc gtaaggaaat cgagcaaatt gccaaggaga ccctcgaagg
      901 caacttgcgt ggtgttttag ccagcctcac gccggagcag atcaacgagg acaaaattgc
      961 ctttgccaaa agtctgctgg aagaggcgga ggatgacctt gagcagctgg gtcaagtcct
     1021 cgatacgctg caagtccaga acatttccga tgaggtcggt tatctctcgg ctagtggacg
     1081 caagcagcgg gctgatctgc agcgagatgc ccgaattgct gaagccgatg cccaggctgc
     1141 ctctgcgatc caaacggccg aaaatgacaa gatcacggcc ctgcgtcgga tcgatcgcga
     1201 tgtagcgatc gcccaagccg aggccgagcg ccggattcag gatgcgttga cgcggcgcga
     1261 agcggtggtg gccgaagctg aagcggacat tgctaccgaa gtcgctcgta gccaagcaga
     1321 actccctgtg cagcaggagc ggatcaaaca ggtgcagcag caacttcaag ccgatgtgat
     1381 cgccccagct gaggcagctt gtaaacgggc gatcgcggaa gcgcgggggg ccgccgcccg
     1441 tatcgtcgaa gatggaaaag ctcaagcgga agggacccaa cggctggcgg aggcttggca
     1501 gaccgctggt gctaatgccc gcgacatctt cctgctccag aagtctagac cagccaggac
     1561 agaaatgcct cgacttcgct gctacccaag gttgccgggt gacgcacacc gtggaaacgg
     1621 atgaaggcac gaacccagtg gacataagcc tgttcggttc gtaagctgta atgcaagtag
     1681 cgtatgcgct cacgcaactg gtccagaacc ttgaccgaac gcagcggtgg taacggcgca
     1741 gtggcggttt tcatggcttg ttatgactgt ttttttgggg tacagtctat gcctcgggca
     1801 tccaagcagc aagcgcgtta cgccgtgggt cgatgtttga tgttatggag cagcaacgat
     1861 gttacgcagc agggcagtcg ccctaaaaca aagttaaaca ttatgaggga agcggtgatc
     1921 gccgaagtat cgactcaact atcagaggta gttggcgtca tcgagcgcca tctcgaaccg
     1981 acgttgctgg ccgtacattt gtacggctcc gcagtggatg gcggcctgaa gccacacagt
     2041 gatattgatt tgctggttac ggtgaccgta aggcttgatg aaacaacgcg gcgagctttg
     2101 atcaacgacc ttttggaaac ttcggcttcc cctggagaga gcgagattct ccgcgctgta
     2161 gaagtcacca ttgttgtgca cgacgacatc attccgtggc gttatccagc taagcgcgaa
     2221 ctgcaatttg gagaatggca gcgcaatgac attcttgctg gtatcttcga gccagccacg
     2281 atcgacattg atctggctat cttgctgaca aaagcaagag aacatagcgt tgccttggta
     2341 ggtccagcgg cggaggaact ctttgatccg gttcctgaac aggatctatt tgaggcgcta
     2401 aatgaaacct taacgctatg gaactcgccg cccgactggg ctggcgatga gcgaaatgta
     2461 gtgcttacgt tgtcccgcat ttggtacagc gcagtaaccg gcaaaatcgc gccgaaggat
     2521 gtcgctgccg actgggcaat ggagcgcctg ccggcccagt atcagcccgt catacttgaa
     2581 gctagacagg cttatcttgg acaagaagaa gatcgcttgg cctcgcgcgc agatcagttg
     2641 gaagaatttg tccactacgt gaaaggcgag atcaccaagg tagtcggcaa ataacccatg
     2701 catgctcact cattaggcac cccaggcttt acactttatg cttccggctc gtatgttgtg
     2761 tggaattgtg agcggataac aatttcacac aggaaacagc tatgaccatg attacgccaa
     2821 gcgcgcaatt aaccctcact aaagggaaca aaagctgggt accgggcccc ccctcgaggt
     2881 cgacggtatc gataagcttg atatcgaatt cctgcagccc ggggatcctc tagagtcgac
     2941 taggaggaat ataaaatgaa aaattgtgtc atcgtcagtg cggtacgtac tgctatcggt
     3001 agttttaacg gttcactcgc ttccaccagc gccatcgacc tgggggcgac agtaattaaa
     3061 gccgccattg aacgtgcaaa aatcgattca caacacgttg atgaagtgat tatgggtaac
     3121 gtgttacaag ccgggctggg gcaaaatccg gcgcgtcagg cactgttaaa aagcgggctg
     3181 gcagaaacgg tgtgcggatt cacggtcaat aaagtatgtg gttcgggtct taaaagtgtg
     3241 gcgcttgccg cccaggccat tcaggcaggt caggcgcaga gcattgtggc gggggtatg
     3301 gaaaatatga gtttagcccc ctacttactc gatgcaaaag cacgctctgg ttatcgtctt
     3361 ggagacggac aggtttatga cgtaatcctg cgcgatggcc tgatgtgcgc cacccatggt
     3421 tatcatatgg ggattaccgc cgaaaacgtg gctaaagagt acggaattac ccgtgaaatg
     3481 caggatgaac tggcgctaca ttcacagcgt aaagcggcag ccgcaattga gtccggtgct
     3541 tttacagccg aaatcgtccc ggtaaatgtt gtcactcgaa agaaaacctt cgtcttcagt
     3601 caagacgaat tcccgaaagc gaattcaacg gctgaagcgt taggtgcatt gcgcccggcc
     3661 ttcgataaag caggaacagt caccgctggg aacgcgtctg gtattaacga cggtgctgcc
     3721 gctctggtga ttatggaaga atctgcggcg ctggcagcag gccttacccc cctggctcgc
     3781 attaaaagtt atgccagcgg tggcgtgccc cccgcattga tgggtatggg gccagtacct
     3841 gccacgcaaa aagcgttaca actggcgggg ctgcaactgg cggatattga tctcattgag
     3901 gctaatgaag catttgctgc acagttcctt gccgttggga aaaacctggg ctttgattct
     3961 gagaaagtga atgtcaacgg cggggccatc gcgctcgggc atcctatcgg tgccagtggt
     4021 gctcgtattc tggtcacact attacatgcc atgcaggcac gcgataaaac gctggggctg
     4081 gcaacactgt gcattggcgg cggtcaggga attgcgatgg tgattgaacg gttgaattaa
     4141 ggaggacagc taaatgaaac tctcaactaa actttgttgg tgtggtatta aaggaagact
     4201 taggccgcaa aagcaacaac aattacacaa tacaaacttg caaatgactg aactaaaaaa
     4261 acaaaagacc gctgaacaaa aaaccagacc tcaaaatgtc ggtattaaag gtatccaaat
     4321 ttacatccca actcaatgtg tcaaccaatc tgagctagag aaatttgatg gcgtttctca
     4381 aggtaaatac acaattggtc tgggccaaac caacatgtct tttgtcaatg acagagaaga
     4441 tatctactcg atgtccctaa ctgttttgtc taagttgatc aagagttaca acatcgacac
     4501 caacaaaatt ggtagattag aagtcggtac tgaaactctg attgacaagt ccaagtctgt
     4561 caagtctgtc ttgatgcaat tgtttggtga aaacactgac gtcgaaggta ttgacacgct
     4621 taatgcctgt tacggtggta ccaacgcgtt gttcaactct ttgaactgga ttgaatctaa
     4681 cgcatgggat ggtagagacg ccattgtagt ttgcggtgat attgccatct acgataaggg
     4741 tgccgcaaga ccaaccggtg gtgccggtac tgttgctatg tggatcggtc ctgatgctcc
     4801 aattgtattt gactctgtaa gagcttctta catggaacac gcctacgatt tttacaagcc
     4861 agatttcacc agcgaatatc cttacgtcga tggtcatttt tcattaactt gttacgtcaa
     4921 ggctcttgat caagtttaca agagttattc caagaaggct atttctaaag ggttggttag
     4981 cgatcccgct ggttcggatg ctttgaacgt tttgaaatat ttcgactaca acgttttcca
     5041 tgttccaacc tgtaaattgg tcacaaaatc atacggtaga ttactatata acgatttcag
     5101 agccaatcct caattgttcc cagaagttga cgccgaatta gctactcgcg attatgacga
     5161 atctttaacc gataagaaca ttgaaaaaac ttttgttaat gttgctaagc cattccacaa
     5221 agagagagtt gcccaatctt tgattgttcc aacaaacaca ggtaacatgt acaccgcatc
     5281 tgtttatgcc gcctttgcat ctctattaaa ctatgttgga tctgacgact tacaaggcaa
     5341 gcgtgttggt ttattttctt acggttccgg tttagctgca tctctatatt cttgcaaaat
     5401 tgttggtgac gtccaacata ttatcaagga attagatatt actaacaaat tagccaagag
     5461 aatcaccgaa actccaaagg attacgaagc tgccatcgaa ttgagagaaa atgcccattt
     5521 gaagaagaac ttcaaacctc aaggttccat tgagcatttg caaagtggtg tttactactt
     5581 gaccaacatc gatgacaaat ttagaagatc ttacgatgtt aaaaaataaa ttcaggaaac
     5641 agaccatgtc catgcaaagt ttagataaga attttcgaca tttatctcgt aaagaaaagt
     5701 tacaacaatt ggttgataag caatggttat cagaagaaca attcgacatt ttactgaatc
     5761 atccattaat cgatgaagaa gtagccaata gtttaattga aaatgtcatc gcgcaaggtg
     5821 cattacccgt tggattatta ccgaatatca ttgtggacga taaggcatat gttgtaccta
     5881 tgatggtgga agagccttca gttgtcgctg cagctagtta tggtgcaaag ctagtgaatc
     5941 agactggcgg atttaaaacg gtatcttctg aacgtattat gataggtcaa atcgtctttg
     6001 atggcgttga cgatactgaa aaattatcag cagacattaa agctttagaa aagcaaattc
     6061 ataaaattgc ggatgaggca tatccttcta ttaaagcgcg tggtggtggt taccaacgta
     6121 tagcgattga tacatttcct gagcaacagt tactatcttt aaaagtattt gttgatacga
     6181 aagatgctat gggcgctaat atgcttaata cgattttaga ggccataact gcatttttaa
     6241 aaaatgaatt tccgcaaagc gacattttaa tgagtatttt atccaatcat gcaacagcgt
     6301 ccgttgttaa agttcaaggc gaaattgatg ttaaagattt agcaaggggc gagagaactg
     6361 gagaagaggt tgccaaacga atggaacgtg cttctgtatt ggcccaagta gatattcatc
     6421 gtgcagcaac acataataaa ggtgttatga atggcataca tgctgttgtt ttagcaacag
     6481 gaaatgatac gcgtggtgca gaagcaagtg cgcatgcata cgcgagtcgt gacggacagt
     6541 atcgtggtat tgctacatgg cgttacgatc aagatcgtca acgattgatt ggtacaattg
     6601 aagtgcctat gacattggca atcgttggcg gtggtacaaa agtattacca attgctaaag
     6661 cttcattaga gctactaaat gtagagtcag cacaagaatt aggtcatgta gttgctgccg
     6721 ttggtttagc gcaaaacttt gcagcatgtc gcgcgcttgt gtcagaaggt attcaacaag
     6781 gtcatatgag tttacaatat aaatcattag ctatcgttgt aggggcaaaa ggtgatgaaa
     6841 ttgctaaagt agctgaagct ttgaaaaaag aaccccgtgc aaatacacaa gcagcggaac
     6901 atattttaca agaaattaga caacaataat tacctgcagg catgcaagct tggctgtttt
     6961 ggcggatgag agaagatttt cagcctgata cagattaaat cagaacgcag aagcggtctg
     7021 ataaaacaga atttgcctgg cggcagtagc gcggtggtcc cacctgaccc catgccgaac
     7081 tcagaagtga aacgccgtag cgccgatggt agtgtggggt ctccccatgc gagagtaggg
     7141 aactgccagg catcaaataa aacgaaaggc tcagtcgaaa gactgggcct ttcgttttat
     7201 ctgttgtttg tcggtgaacg ctctcctgag taggacaaat ccgccgggag cggatttgaa
     7261 cgttgcgaag caacggcccg gagggtggcg ggcaggacgc ccgccataaa ctgccaggca
     7321 tcaaattaag cagaaggcca tcctgacgga tggccttttt gcgtttctac aaactctttt
     7381 gtttattttt ctaaatacat tcaaatatgt atccgctcat gacctaggtc tcgagtccct
     7441 gctcgtcacg ctttcaggca ccgtgccaga tatcgacgtg gagtcgatca ctgtgattgg
     7501 cgaaggggaa ggcagcgcta cccaaatcgc tagcttgctg gagaagctga aacaaaccac
     7561 gggcattgat ctggcgaaat ccctaccggg tcaatccgac tcgcccgctg cgaagtccta
     7621 agagatagcg atgtgaccgc gatcgcttgt caagaatccc agtgatcccg aaccatagga
     7681 aggcaagctc aatgcttgcc tcgtcttgag gactatctag atgtctgtgg aacgcacatt
     7741 tattgccatc aagcccgatg gcgttcagcg gggtttggtc ggtacgatca tcggccgctt
     7801 tgagcaaaaa ggcttcaaac tggtgggcct aaagcagctg aagcccagtc gcgagctggc
     7861 cgaacagcac tatgctgtcc accgcgagcg cccttcttc aatggcctcg tcgagttcat
     7921 cacctctggg ccgatcgtgg cgatcgtctt ggaaggcgaa ggcgttgtgg cggctgctcg
     7981 caagttgatc ggcgctacca atccgctgac ggcagaaccg ggcaccatcc gtggtgattt
     8041 tggtgtcaat attggccgca acatcatcca tggctcggat gcaatcgaaa cagcacaaca
     8101 ggaaattgct ctctggttta gcccagcaga gctaagtgat tggacccca cgattcaacc
     8161 ctggctgtac gaataaggtc tgcattcctt cagagagaca ttgccatgcc g
//
```